

The Genetic Basis of phage susceptibility, cross-resistance and host-range in *Salmonella*

Benjamin A. Adler^{1,2,3}, Alexey E. Kazakov⁴, Crystal Zhong², Hualan Liu⁴, Elizabeth Kutter⁵, Lauren M. Lui⁴, Torben N. Nielsen⁴, Heloise Carion², Adam M. Deutschbauer^{4,6}, Vivek K. Mutalik^{3,4*}, Adam P. Arkin^{2,3,4*}

1. The UC Berkeley-UCSF Graduate Program in Bioengineering, Berkeley, California, United States
2. Department of Bioengineering, University of California, Berkeley, Berkeley, California, United States
3. Innovative Genomics Institute, University of California, Berkeley, Berkeley, United States
4. Environmental Genomics and Systems Biology Division, Lawrence Berkeley National Laboratory, Berkeley, California, United States
5. The Evergreen State College, Olympia, Washington, United States
6. Department of Plant and Microbial Biology, University of California, Berkeley, Berkeley, California, United States

* Correspondence:

Vivek K. Mutalik (vkmutalik@lbl.gov), Adam P. Arkin (aparkin@lbl.gov)

29 **Summary**

30

31 Though bacteriophages (phages) are known to play a crucial role in bacterial fitness and
32 virulence, our knowledge about the genetic basis of their interaction, cross-resistance and host-
33 range is sparse. Here, we employed genome-wide screens in *Salmonella enterica* serovar
34 Typhimurium to discover host determinants involved in resistance to eleven diverse lytic phages
35 including 4 new phages isolated from a therapeutic phage cocktail. We uncovered 301 diverse
36 host factors essential in phage infection, many of which are shared between multiple phages
37 demonstrating potential cross-resistance mechanisms. We validate many of these novel
38 findings and uncover the intricate interplay between RpoS, the virulence-associated general
39 stress response sigma factor and RpoN, the nitrogen starvation sigma factor in phage cross-
40 resistance. Finally, the infectivity pattern of eleven phages across a panel of 23 genome
41 sequenced *Salmonella* strains indicates that additional constraints and interactions beyond the
42 host factors uncovered here define the phage host range.

43

44

45

46

47

48

49

50 Introduction

51 There is increasing evidence that bacteriophages are a critical feature of microbial ecology,
52 evolution, virulence and fitness(Abedon, 2009; Breitbart and Rohwer, 2005; Koskella and
53 Taylor, 2018; Shkoporov and Hill, 2019; Suttle, 2007). However, knowledge about the molecular
54 and genetic determinants of host-phage interactions and how they vary across the populations
55 of both are sparse even in otherwise well-studied model systems(Brüssow, 2013; de Jonge et
56 al., 2019; Nobrega et al., 2018; Rostøl and Marraffini, 2019; Samson et al., 2013; Weitz et al.,
57 2013; Young and Gill, 2015). This derives, in part, from the technological limitations to resolve
58 the incredible specificity and the complex suite of bacterial mechanisms that confer both
59 resistance and sensitivity to the phage(De Smet et al., 2017; Nobrega et al., 2018; Young and
60 Gill, 2015). A given bacterial host is likely to be susceptible to multiple phages, while a given
61 phage may infect a specific array of hosts and their variants. There are few, if any, studies that
62 map these mechanisms across phages and hosts, their interdependencies, and how variations
63 in these mechanisms encode tradeoffs in host and phage fitness under different
64 conditions(Calendar, 2012; Casjens and Hendrix, 2015; De Smet et al., 2017; Karam and
65 Drake, 1994; Molineux, 2002). However, this information is critical to an understanding of
66 microbial ecology and possibly exploiting the predator-prey dynamics for applications(Campbell,
67 2003; Díaz-Muñoz and Koskella, 2014; Lenski, 1988; Mirzaei and Maurice, 2017).

68 Knowledge of phage susceptibility and resistance determinants underlies a number practical
69 applications of phages. These applications span the use of phages and their combinations as
70 biocontrol agents to improve water quality, decontaminate food, protect agricultural yield, and
71 defend and improve human health(Gordillo Altamirano and Barr, 2019; Keen and Adhya, 2015;
72 Kortright et al., 2019; Pirnay and Kutter, 2020). For example, because of the apparent ubiquity
73 of lytic phage with high host specificity for nearly any known pathogenic bacterial strain, phages
74 may provide a powerful alternative or adjuvant to antibiotic therapies. The development of such
75 therapeutic phage formulations is pressing due to the alarming rise of antibiotic
76 resistance(Gordillo Altamirano and Barr, 2019; Keen and Adhya, 2015; Kortright et al., 2019;
77 Young and Gill, 2015). By characterizing the genetic basis of a bacterium's susceptibility and
78 resistance to a given phage and the pattern of cross-resistance or cross-sensitivity with other
79 phages, we can uncover evolutionary trade-offs on bacteria-phage interactions. These insights
80 could also identify knowledge-gaps in our understanding of the host-range of a phage and offer
81 therapeutic solutions to recalcitrant infections(Chan et al., 2016; Gordillo Altamirano et al., 2021;
82 Mangalea and Duerkop, 2020; Shin et al., 2012; Trudelle et al., 2019; Wright et al., 2018). For
83 instance, by leveraging phages that target different receptors, combinations of phages or phage
84 cocktails can be rationally formulated to both extend the host range and limit the rate of
85 resistance emergence(Bai et al., 2019; Chan et al., 2013; Kortright et al., 2019; Tanji et al.,
86 2004; Yen et al., 2017). Such strategies can be further augmented by selecting phages that
87 specifically bind to bacterial virulence or antibiotic resistance factors to benefit from evolutionary
88 trade-offs in rational therapeutic outcomes (Chan et al., 2013; Kortright et al., 2019).

89 Compared to other antimicrobials, characterization of infectivity and cross-resistance between a
90 panel of phages has been limited to a few model organisms and remained phenomenological
91 until recently(Hudson et al., 1978; Lindberg and Hellerqvist, 1971; Marti et al., 2013; Samuel et
92 al., 1999; Tu et al., 2017; Wright et al., 1980). The advent of genome-wide saturated transposon
93 sequencing (Bohm et al., 2018; Chan and Turner, 2020; Christen et al., 2016; Cowley et al.,
94 2018; Pickard et al., 2013) and the corresponding DNA bar-code based modifications has
95 enabled the high-throughput and low cost genome-scale screening for the genetic determinants
96 of these phenomena(Carim et al., 2020; Mutalik et al., 2019, 2020; Rousset et al., 2018;
97 Wetmore et al., 2015). Since this economically permits the independent screening of many

98 phages against a host library, it is now possible to determine and compare the genes that affect
99 the successful infection of one or more phages. These insights further suggest possible
100 mechanisms of cross-resistance (ie single mutations that confer resistance to multiple phages)
101 and collateral-sensitivity (ie single mutations that cause resistance to one phage while
102 sensitizing to another phage) that might arise when the host is naturally exposed to different
103 combinations of these phages in the environment. As an example of this approach, we recently
104 employed a high-throughput genetic screening platform to characterize the phage resistance
105 landscape in *Escherichia coli* (*E.coli*) at an unprecedented scale(Mutalik et al., 2020). However,
106 the scale and benefits of these technologies have not yet been realized outside of such model
107 organisms, where bacterial physiology and phage-host interactions can be dramatically
108 different. Here, we employ a genome-wide loss-of-function screening technology to discover the
109 genetic determinants of phage susceptibility in *Salmonella enterica*, a globally important
110 infectious bacteria whose variants are responsible for the vast majority of bacterial food-borne
111 infections with an annual cost of \$3.7B dollars in 2013(Macculloch et al., 2015). Though
112 *Salmonella enterica* serovar Typhimurium (*S. Typhimurium*) has been used in the past as a
113 model host to study phage infections(Graña et al., 1985; Lee et al., 2013; Lindberg and
114 Hellerqvist, 1971; MacPhee et al., 1975; Marti et al., 2013; Schwartz, 1980; Wilkinson et al.,
115 1972; Wright et al., 1980), most *Salmonella* phages including therapeutically employed phage
116 formulations have limited characterization regarding target receptors and host resistance
117 mechanisms (Bai et al., 2019; Gao et al., 2020; Islam et al., 2019; McCallin et al., 2018;
118 Petsong et al., 2019; Zschach et al., 2015). With increased numbers of *Salmonella* infections
119 that are resistant to antibiotics and displaying increased virulence(Medalla et al., 2016; (u.s.)
120 and Centers for Disease Control and Prevention (U.S.), 2019), it is imperative to characterize
121 phages and their resistance patterns to enable their rational use as diagnostic and antimicrobial
122 agents.

123 In this study, we use a *S. enterica* serovar Typhimurium (*S. Typhimurium*) LT2 derivative that
124 serves as a genetically-accessible model for a clade of *Salmonella* responsible for food-borne
125 enteric infections in humans. Using a barcoded transposon mutant library, we identified bacterial
126 genes whose loss confers altered sensitivity to 11 diverse double-stranded DNA phages
127 including 4 new phages isolated from a therapeutic phage cocktail. Our screens identified
128 known (and proposed new) receptors and also yielded novel host factors important in phage
129 infection, some of which we validate using single-gene deletion strains. Our genetic analysis
130 allowed high resolution mapping of phage interactions with diverse cell surface components and
131 the operation of specific global regulatory systems that mediate specific metabolisms (e.g. *rpoM*)
132 or virulence and stress response (e.g. *rpoS*). The diversity of cellular processes that influence
133 sensitivity to phage suggest that there may be multiple routes for cross-resistance and cross-
134 sensitivity to emerge due to phage exposure in the environment or when used as therapeutic
135 cocktails. Finally, to assess if phage susceptibility and phage host-range can be predicted
136 based on the genetic determinants uncovered by our screens, we measured and analyzed
137 phage infectivity against a panel of 23 *S.Typhimurium* strains representative of naturally
138 occurring genetic diversity and phage infectivity.

139

140 **Results**

141

142 **Identifying *Salmonella* genes involved in resistance to 11 diverse phages**

143 We previously established a high-throughput approach to assay gene fitness using genome-
144 wide, random barcoded transposon sequencing (RB-TnSeq) (Price et al., 2018; Wetmore et al.,
145 2015). To systematically characterize phage infectivity pathways in *Salmonella*, we first

146 constructed an RB-TnSeq library in *S. Typhimurium* LT2 derivative strain MS1868 (Graña et al.,
147 1985) (Methods). As an LT2-derived strain, *S. Typhimurium* MS1868 benefits from a long
148 history of *Salmonella* phage-host genetic interaction studies and well-characterized phage-
149 resistant genotypes (Hudson et al., 1978; Lindberg and Hellerqvist, 1971; Marti et al., 2013;
150 Samuel et al., 1999; Tu et al., 2017; Wilkinson et al., 1972; Wright et al., 1980). In addition, *S.*
151 *Typhimurium* MS1868 is a restriction-minus genetic background (Graña et al., 1985), which
152 would potentially help uncover additional phage resistance factors by expanding the number of
153 phages infectious to the RB-TnSeq library. After transposon mutagenesis, we obtained a 66,996
154 member pooled library consisting of transposon-mediated disruptions across 3,759 of 4,610
155 genes, with an average of 14.8 disruptions per gene (median 12) (Figure 1A). We note that our
156 library does not have sufficient coverage of some likely non-essential genes that are likely to play an
157 important role in phage infection, for example *igaA* (Cho et al., 2014; Mariscotti and Garcia-del
158 Portillo, 2009; Mutalik et al., 2020). Additional details for the composition of the *S. Typhimurium*
159 MS1868 library and comparison to a related single-gene-deletion library (Porwollik et al., 2014)
160 can be found in Table S1 and Dataset S1.

161
162 We collected 11 lytic, dsDNA *Salmonella* phages, some of which are currently employed in
163 therapy and diagnostics. These phages are diverse, representing 5 of the 9 major dsDNA phage
164 families currently listed by the International Committee on Taxonomy of Viruses (ICTV): 3 from
165 Myoviridae (FelixO1, S16, and Savina_GE), 1 from Podoviridae (P22), 4 from Autographiviridae
166 (Br60, Ffm, Shishito_GE, and SP6), 2 from Siphoviridae (Chi, and Reaper_GE), and 1 from
167 Demereciviridae (Aji_GE). Though the receptors for 4 of the phages investigated here, Chi,
168 FelixO1, P22 (obligately lytic mutant), and S16 are relatively well-studied, (Graña et al., 1985;
169 Lee et al., 2013; Lindberg and Hellerqvist, 1971; MacPhee et al., 1975; Marti et al., 2013;
170 Schwartz, 1980; Wilkinson et al., 1972; Wright et al., 1980), only P22 phage has been subjected
171 to a genome-wide genetic screen (Bohm et al., 2018). Additionally, Br60, Ffm, and SP6 have
172 suspected host-factor requirements for their infectivity cycle but otherwise have not been
173 extensively studied (Gebhart et al., 2017; Lindberg and Hellerqvist, 1971; Tu et al., 2017). This
174 panel of 11 phages also consists of 4 newly isolated phages from a commercial phage-cocktail
175 preparation from the Republic of Georgia (see Methods, Dataset S7): Aji_GE_EIP16 (Aji_GE),
176 Reaper_GE_8C2 (Reaper_GE), Savina_GE_6H2 (Savina_GE), and Shishito_GE_6F2
177 (Shishito_GE). All 11 phages except 3 (Br60, Ffm and Shishito_GE) infect wild-type *S.*
178 *Typhimurium* LT2 MS1868, which has an intact O-antigen (known as 'smooth-LPS'). Br60, Ffm
179 and Shishito_GE phages were grown using a 'rough-LPS' mutant strain of *Salmonella* which
180 consists of only core LPS (see Methods). Thus, the phage panel used here contains phages
181 that either bind to smooth or rough LPS strains and allows comparison of the key host factors
182 important in their infectivity cycles.

183
184 To identify *Salmonella* genes important for phage infection, we challenged the *S. Typhimurium*
185 mutant library with each of the 11 dsDNA lytic phages (Table 1) at multiplicities of infection ≥ 2
186 in both planktonic and non-competitive solid plate fitness experiments, and collected the
187 surviving phage-resistant strains post incubation (Figure 1A, Methods). From samples collected
188 before and after phage incubation, we sequenced the 20 base pair DNA barcodes (i.e. BarSeq)
189 associated with each transposon mutant. We then calculated strain and gene fitness scores as
190 the relative log₂-fold-change of barcode abundances before versus after phage selection, as

191 previously described (Mutalik et al., 2020; Price et al., 2018; Wetmore et al., 2015) (Figure 1A,
192 Methods). Thus, in this study, a high positive fitness score indicates loss-of-function mutants in
193 *Salmonella* that are resistant to phage infection. We observed very strong phage selection
194 pressures during these competitive fitness experiments, consistent with our earlier observations
195 (Mutalik et al., 2020), and thus we mostly limited our analysis to positive fitness scores. As
196 expected with our MS1868 library primarily consisting of O-antigen positive mutants, the vast
197 majority of gene disruptions in MS1868 showed no significant fitness benefit against rough-LPS
198 binding Br60, Ffm and Shishito_GE phages. However, we noticed strong fitness defects in
199 many of the LPS and O-antigen mutants in our library (Figure 1BC, Dataset S4), consistent with
200 optimal adsorption and infection in O-antigen-defective *Salmonellae*.

201
202 In aggregate, we performed 42 genome-wide RB-TnSeq assays across liquid and solid growth
203 formats and discovered 301 phage-gene interactions (with 184 unique gene hits) that are
204 important for phage infection across the 11 phages studied (Figure 1BC, Datasets S2 and S4).
205 Though solid plate assay results were largely consistent with planktonic assays, some resulted
206 in genes with stronger fitness effects. Across all fitness experiments, we observed at least one
207 gene with a high fitness score (except 3 phages that infect rough-LPS strains), affirming the
208 successful competitive growth of mutants under phage selection. Some *Salmonella* phages
209 show enrichment of strains with disruptions in multiple genes, while other phages enrich strains
210 with disruptions in a more limited number of genes (Figure 1B). For example, we observed 98
211 genes enriched after Chi phage challenge and 73 high-scoring genes after Felix O1 challenge,
212 yet only 7 high-scoring genes after S16 phage challenge. As expected in any phage selection
213 experiment, we observed enrichment of genes that encode components of the cell envelope.
214 Nonetheless, we also identified dozens of genes that encode cytoplasmic components not
215 previously associated with phage resistance. To further categorize the genetic basis of phage
216 resistance, we manually classified all identified genes with high fitness values into broad-
217 functional categories: core-LPS and O-antigen biosynthesis, motility, secondary messengers,
218 transcription factors and other metabolism (Figure 1C). These results demonstrate that genes
219 downstream from phage receptors are important for phage infectivity.

220

221 **Both receptor and non-receptor host factors are involved in phage infection**

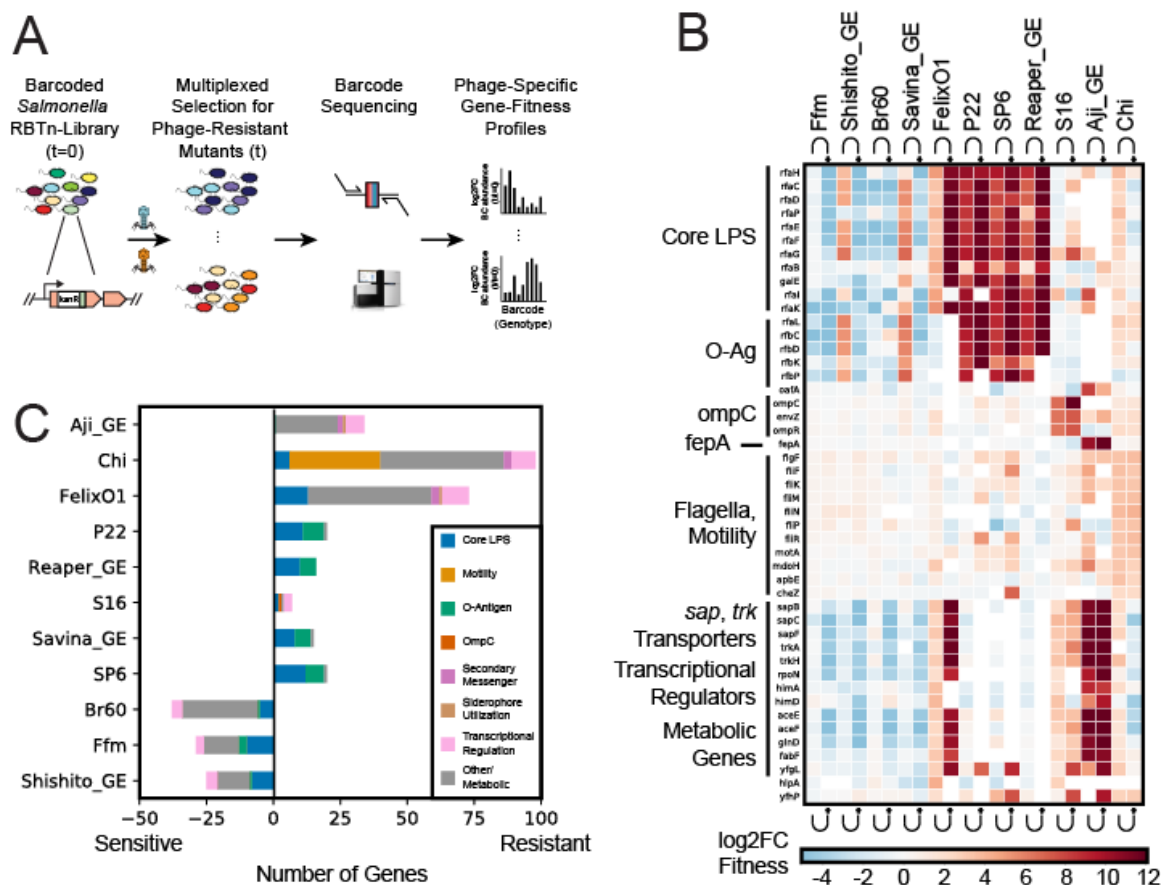
222 A key-determining step in the phage infectivity cycle is the interaction of phages with any
223 bacterial cell surface-exposed molecules or receptors. Consequently, any changes in the
224 structure or level of these surface-exposed molecules that accompany resistance to specific
225 phages are usually assigned a function of phage receptor. To confirm the effectiveness of our
226 genetic screen, we looked for receptors that are known for a few of the phages used in this work
227 (Bohm et al., 2018; Hudson et al., 1978; Lindberg and Hellerqvist, 1971; MacPhee et al., 1975;
228 Marti et al., 2013; Samuel et al., 1999). Indeed, in agreement with published data available for
229 FelixO1, P22, Chi, SP6 and S16 phages, we found high fitness scores for candidate receptor
230 genes with >1,000 fold enrichment of transposon mutants. These included genes encoding
231 protein receptors such as *ompC* (outer membrane porin C) for S16 and flagellar body for Chi
232 phage, while LPS and O-antigen biosynthesis genes for P22, SP6 and FelixO1 phages (Figure
233 1C). Our results are also largely consistent with a recent genome-wide screen in *Salmonella*
234 against P22 infection (Bohm et al., 2018). Though O-antigen and outer core GlcNAc (the
235 biosynthetic product of RfaK) have been known as SP6 and as FelixO1 phage receptors
236 respectively (Hudson et al., 1978; Lindberg and Hellerqvist, 1971; Marti et al., 2013; Samuel et
237 al., 1999; Tu et al., 2017; Wilkinson et al., 1972; Wright et al., 1980), our genome-wide screens
238 provided an array of additional, non-receptor genes as target loci for phage resistance selection.

239 A detailed description and analysis of outer membrane components such as LPS required for
240 these phages can be found in Text S1.

241
242 In addition to the genes coding for phage receptors, our genetic screens also uncovered high-
243 scoring genes that are known to be involved in the regulation of target receptors. For example,
244 deletion of the EnvZ/OmpR two component system involved in the regulation of *ompC* and gene
245 products involved in the regulation of cellular motility (*nusA*, *tolA*, *cyaA* and guanosine
246 penta/tetraphosphate ((p)ppGpp) biosynthesis and metabolism all showed high fitness scores
247 in the presence of S16 and Chi phages, respectively (Graña et al., 1985; Lee et al., 2013;
248 Lindberg and Hellerqvist, 1971; MacPhee et al., 1975; Marti et al., 2013; Schwartz, 1980;
249 Wilkinson et al., 1972; Wright et al., 1980). These high-scoring gene candidates were previously
250 not known to be associated with phage resistance in *Salmonella*. Other than the phages
251 mentioned above that bind to surface components of smooth-LPS *Salmonellae*, we also
252 screened Br60 and Ffm phages, which are known to strictly infect rough-LPS strains and not
253 bind to smooth WT MS1868 parental strain (as O-antigen structure probably occludes their
254 native receptor) (Gebhart et al., 2017; Lindberg and Hellerqvist, 1971; Tu et al., 2017). As our
255 MS1868 library primarily consists of O-antigen positive mutants, the vast majority of gene
256 disruptions in MS1868 showed no significant fitness benefit against these phages. However, we
257 noticed strong negative scores for many of the LPS and O-antigen mutants in our library
258 (Dataset S4), indicating these strains have rough LPS phenotype and are sensitive to Br60 and
259 Ffm phages. As an additional resource, we determined the specific rough-LPS requirements for
260 these phages using an O-antigen deficient library and individual mutant susceptibility assays
261 (Text S1 - Extended Results: Uncovering Host-Factors of Rough-LPS Requiring Phages Br60,
262 Ffm, and Shishito_GE).

263
264 Among the four newly isolated phages (Reaper_GE, Savina_GE, Aji_GE and Shishito_GE),
265 Reaper_GE showed strict requirements for O-antigen including a complete LPS (Figure 2B),
266 while Savina_GE primarily showed dependency on O-antigen followed by inner core mutants,
267 and outer core mutants (Figure 2B, Dataset S4). For T5-like phage Aji_GE, both *fepA* (TonB-
268 dependent enterobactin receptor) and *oafA* (O-antigen acyltransferase) showed high fitness
269 scores. OafA performs an acetylation reaction on the abequose residue to create the O5-
270 antigen serotype in LT2-derived strains (Slauch et al., 1996), and probably enhances infection
271 via gaining access to the FepA-TonB complex. Related phenomena have been observed for
272 other *Demerecviiridae*, where other O-antigen modifications facilitated increased phage
273 susceptibility (Heller and Braun, 1982; Kim and Ryu, 2012). Finally, similar to Br60 and Ffm
274 phages isolated on rough-LPS *Salmonella*, Shishito_GE displayed strong host fitness defects in
275 many of the LPS and O-antigen mutants in our library.

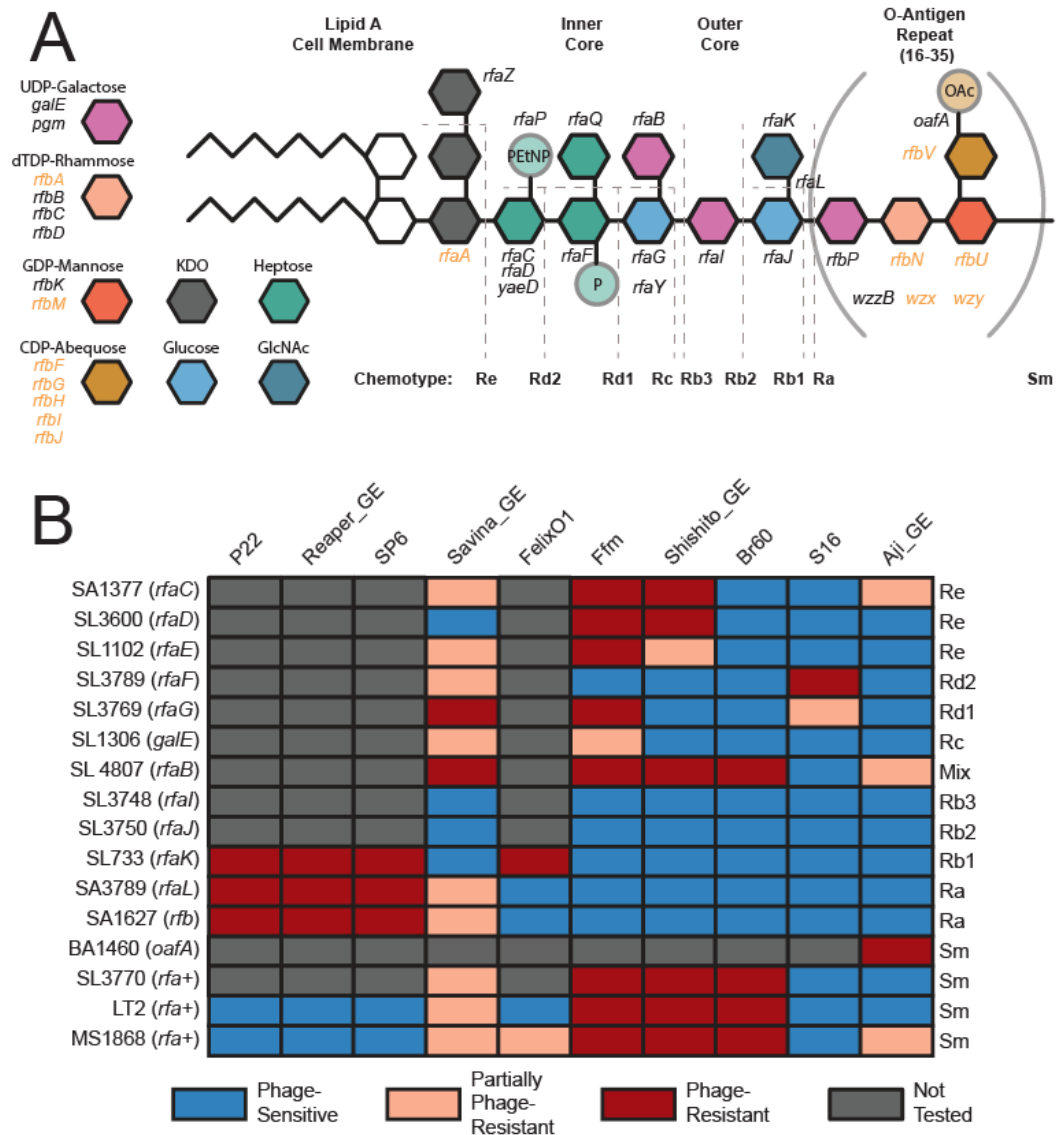
276
277
278
279



280
281
282 **Figure 1. Genome-wide screen to identify host factors involved in phage infection.** (A) Overview of
283 pooled fitness assays. For additional details, see methods. Briefly, for each experiment, *S. Typhimurium*
284 RB-TnSeq library was exposed to a high MOI of one of eleven dsDNA *Salmonella* phages. Strains were
285 tracked by quantifying the abundance of DNA barcodes associated with each strain by Illumina
286 sequencing. Phage-specific gene fitness profiles were calculated by taking the log₂-fold-change of
287 barcode abundances post- (t) to pre- (t=0) phage predation. High fitness scores indicate that loss of
288 genetic function in *Salmonella* confers fitness against phage predation. (B) Heatmap of top 10 high-
289 confidence gene scores per phage are shown (many genes are high-confidence hits to multiple phages).
290 Both planktonic and solid plate data are shown. Three rough-LPS binding phages Br60, Ffm, and
291 Shishito_GE do not infect wild-type MS1868, but can infect specific MS1868 mutants, overall showing
292 negative fitness values in our screen. Noncompetitive, solid agar growth experiments are marked
293 with a (*). (C) Total number of high-scoring genes per phage and their functional role. Input data for
294 Figures 1B and 1C is found in Dataset S4 and can be recreated using Supplementary Code - Figure1BC.

295
296
297
298 To validate some of the top phage resistance phenotypes from our genetic screens, we used an
299 established collection of *Salmonella* mutant strains in addition to the construction of deletion
300 strains (Table S5)(Roantree et al., 1977; Sanderson et al., 1974). To confirm the role of OafA
301 and TonB-dependent enterobactin receptor FepA (FepA-TonB complex) on Aji_GE infectivity,
302 we constructed strains with deletions in *oafA*, *fepA*, and *tonB* (Methods). Aji_GE phage plaque
303 assays on these strains confirmed the essentiality of OafA and both FepA-TonB in infection
304 (Figures 2 and S17). For phages that showed stringent requirements of O-antigen and LPS, we

305 used an established chemotype-defined LPS mutant panel in a *S. Typhimurium* strain
306 background that is closely related to our LT2 derivative (Figures 2, S5-S11, and S13-S15, Table
307 S5, Methods). Our phage infectivity results on the LPS chemotype panel are in agreement with
308 earlier published data for some of the phages used in this work (Bohm et al., 2018; Lindberg
309 and Hellerqvist, 1971; Marti et al., 2013; Mutalik et al., 2020; Wright et al., 1980) and consistent
310 with our high-throughput genetic screens for all phages (Figure 1B). For example, LPS
311 chemotype panel data confirmed the strict requirements for O-antigen including a complete LPS
312 for Reaper_GE infectivity. We confirmed that Savina_GE most efficiently infects strains with an
313 incomplete outer core, but less so against strains without O-antigen or strains missing outer
314 core entirely (Figures 2 and S9). This result indicates Savina_GE preferentially employs LPS as
315 a receptor, but branched LPS residues such as those added by *rfaK* and O-antigen biosynthesis
316 probably hinder efficient adsorption. Though OafA activity is important for Aji_GE infection
317 (Figure 2, BA1460), the acetylation provided by OafA activity does not seem to be critical in the
318 absence of complete LPS and O-antigen as those mutants showed significant infection (Figures
319 2, S3, S11, and S17). The plaque assays of Shishito_GE on the LPS mutant panel confirmed
320 that, like phages Br60 and Ffm, it only infects rough-LPS strains of *Salmonella* (Figures 2, S4,
321 and S13-S15). As the inner and outer core LPS structure of *S. Typhimurium* is conserved in *E.*
322 *coli* K-12, we confirmed these observations using data from an RB-TnSeq library of *E. coli* K-12
323 (Figure S4, Text S1, Methods). In summary, the combination of our high-throughput genetic
324 screen and assays on single-gene deletion strains provided higher resolution mapping of O-
325 antigen, LPS or protein receptor requirement for all 11 phages in *Salmonella* (a detailed
326 description for each phage is in Text S1).
327
328



329 **Figure 2:** Validation of LPS-moiety requirements for *Salmonella* phages (A) Overview of O5 *S.*
 330 Typhimurium LPS and O-antigen biosynthesis. The four sugars in brackets comprise the O-antigen, which
 331 repeats 16-35 times per LPS molecule under standard growth conditions. Key for non-essential LPS and
 332 O-antigen precursor biosynthesis genes are described to the right. Genes covered in our library and used
 333 for analysis are written in black. Genes not covered in our library, and thus not analyzed in this study are
 334 written in orange. (B) Infectivity matrix using a previously established *Salmonella* LPS panel (Table S5).
 335 The identity of the LPS chemotype corresponding to specific mutation is presented in (A). sm stands for
 336 smooth-LPS chemotype. Data for this figure is aggregated from Figures S5-S11, S13-S15, and S17.
 337
 338
 339
 340
 341
 342

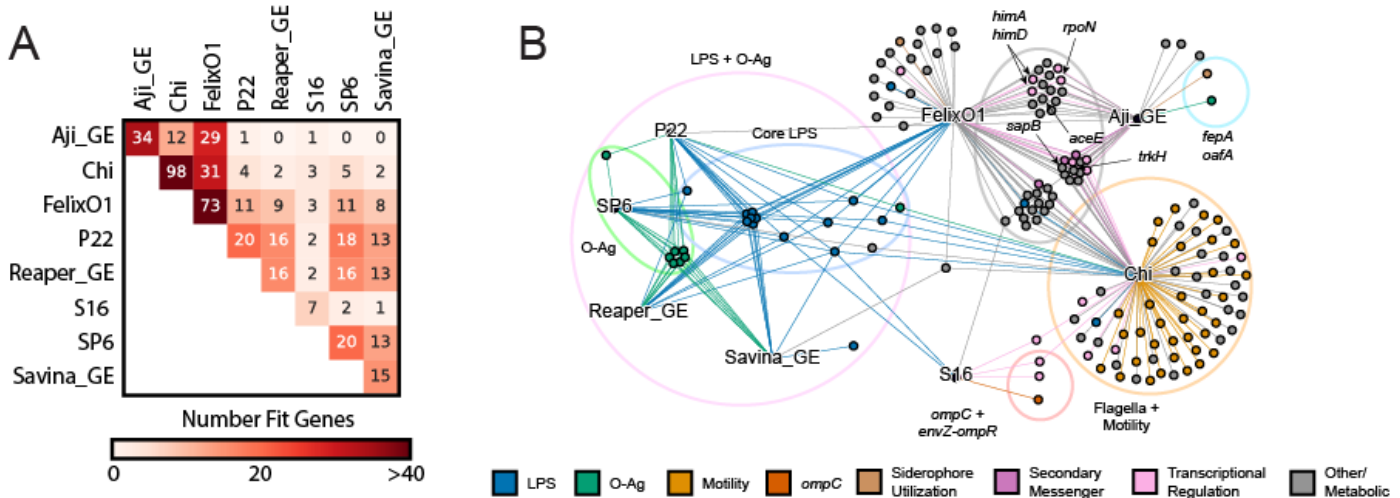
Discovery of Novel Cross-Resistant Genotypes Between Diverse Phages

343 Next, we looked at the number and pattern of high-fitness scoring genes against our panel of
344 phages to identify similarity in infectivity cycles and commonality in genetic barriers leading to
345 phage cross-resistance. The most studied mode of resistance between phages is when they
346 share a common receptor (for example, phages binding to LPS), and any modification in the
347 common receptor yields cross-resistance to those phages (Chan and Turner, 2020; Mutalik et
348 al., 2020; Shin et al., 2012; Wright et al., 2018, 2019). Though it is possible that other host
349 factors are important for the infectivity cycle of different phages and can impart phage cross-
350 resistance phenotypes, it remains a challenge to identify such non-receptor host factors and
351 their role in phage infection. Thus they are not widely reported, nonetheless in the context of
352 phage cross-resistance. For example, mutations in global transcriptional regulators can impart
353 broad resistance to diverse phages that bind to different receptors, but have been proposed to
354 impart higher fitness costs which probably explain their lower frequency of emergence (Betts et
355 al., 2016; Díaz-Muñoz and Koskella, 2014; Hesse et al., 2020; Mutalik et al., 2020; Wright et al.,
356 2018, 2019).

357
358 To gain more insights into phage cross-resistance, we compared the genes that show high-
359 fitness scores across the 8 smooth-LPS binding phages screened in our study (Figure 3AB).
360 The pair-wise comparison between any two phages indicated that, there is a wide range of
361 shared high-fitness scoring genes. As expected, phages that bind to the same receptor shared
362 many high-scoring genes indicating potential cross-resistance between them. For example, P22
363 SP6 and Reaper_GE bind to O-antigen and share many common high scoring hits. Conversely,
364 there are instances of no high-fitness scoring genes shared between phages employing
365 different receptors (for example, between Aji_GE and the O-antigen requiring phages
366 Reaper_GE, SP6 and Savina_GE) (Figure 3A). Unexpectedly, we also observed instances of
367 shared genes across phages that bind to different receptors, and point to a role played by the
368 non-receptor host factors (Figure 3). For example, Aji_GE and FelixO1 have different receptors,
369 yet they share a large number of high-fitness scoring genes, indicating potential cross-
370 resistance independent of their primary receptors (Figures 1 and 3). Out of 52 non-receptor
371 genes conferring resistance to FelixO1 and 32 non-receptor genes conferring resistance to
372 Aji_GE, 29 were common to Aji_GE and FelixO1. These common non-receptor host factors
373 appear to play diverse roles, and the functions they encode include disruptions across central
374 metabolism (*aceEF*, *pta*, *ackA*, *fabF*), amino acid biosynthesis and regulation (*rpoN*, *glnDLG*,
375 *ptsIN*, *aroM*), global regulation (*himAD*, *crp*, *rpoN*, *lon*, *arcB*), ion transport (*trkAH*), peptide
376 transport (*sapABC*), secondary messenger signaling (*gppA*, *cyaA*), translation (*trpS*), and
377 other genes with less clear functions (*nfuA*, *yfgL*, *ytfP*). Some of these genes were recently
378 implicated as host-factors in phage resistance in related organisms (Cowley et al., 2018;
379 Goosen and Putte, 1995; Wright et al., 2018), though their role in phage cross-resistance and
380 mechanisms were not determined. For example, *trk*, *sap*, *ace* and *rpoN* were recently
381 associated with diverse phage resistance in *E. coli* (Cowley et al., 2018; Kortright et al., 2020)
382 and *P. aeruginosa* (Wright et al., 2018). *himA* and *himD* (i.e. integration host factor subunits
383 alpha and beta) are known to be involved in temperate phage infection pathways, though not
384 shown for obligately lytic phages such as Aji_GE and FelixO1 (Goosen and Putte, 1995).

385
386 To investigate if these mutants indeed display cross-resistance to both Aji_GE and FelixO1, we
387 selected a few top scoring genes to study further: *trkH*, *sapB*, *aceE*, *rpoN*, *himA*, and *himD*. For
388 each of these 6 genes, we created individual mutants (Methods) and assessed Aji_GE and
389 FelixO1 phage infectivity. Indeed, the *trkH*, *sapB*, *aceE*, *rpoN*, *himA* and *himD* mutants showed
390 increased resistance to both FelixO1 and Aji_GE (Figures S19-S20). Consistent with prior
391 reports of high fitness costs being associated with non-receptor phage cross-resistant mutants

392 (Wright et al., 2018), mutants in *aceE*, *rpoN*, and *himA* displayed significant growth defects
 393 during planktonic growth, but were sufficiently fit to be uncovered in our screens. Some of these
 394 genes (for example, potassium transporter Trk and nitrogen assimilation sigma factor RpoN) are
 395 known to play an important ecological role in *Salmonella* virulence and fitness in infection
 396 contexts (Klose and Mekalanos, 1997; Su et al., 2009), indicating these phage resistance loci
 397 may exhibit an evolutionary trade-off with virulence.



398
 399 **Figure 3: Cross-resistance is common between *Salmonella* phages.** (A) Summary of cross-
 400 resistance patterns between phages observed in our screens. Heatmap color represents the total number
 401 of shared gene disruptions in *S.Typhimurium* that yield resistance to both phages. (B) Mixed-node
 402 network graph showing connections between phage nodes (text labels, black) and gene nodes (colored
 403 nodes). A gene node is connected to a phage node if disruptions in that gene gave high fitness against
 404 that phage (Dataset S4). Gene nodes are colored by encoded function. Notable gene function groupings
 405 and genes are additionally highlighted. Figures 3A and 3B are created from Dataset S4 using
 406 Supplemental Code - Figure3AB.

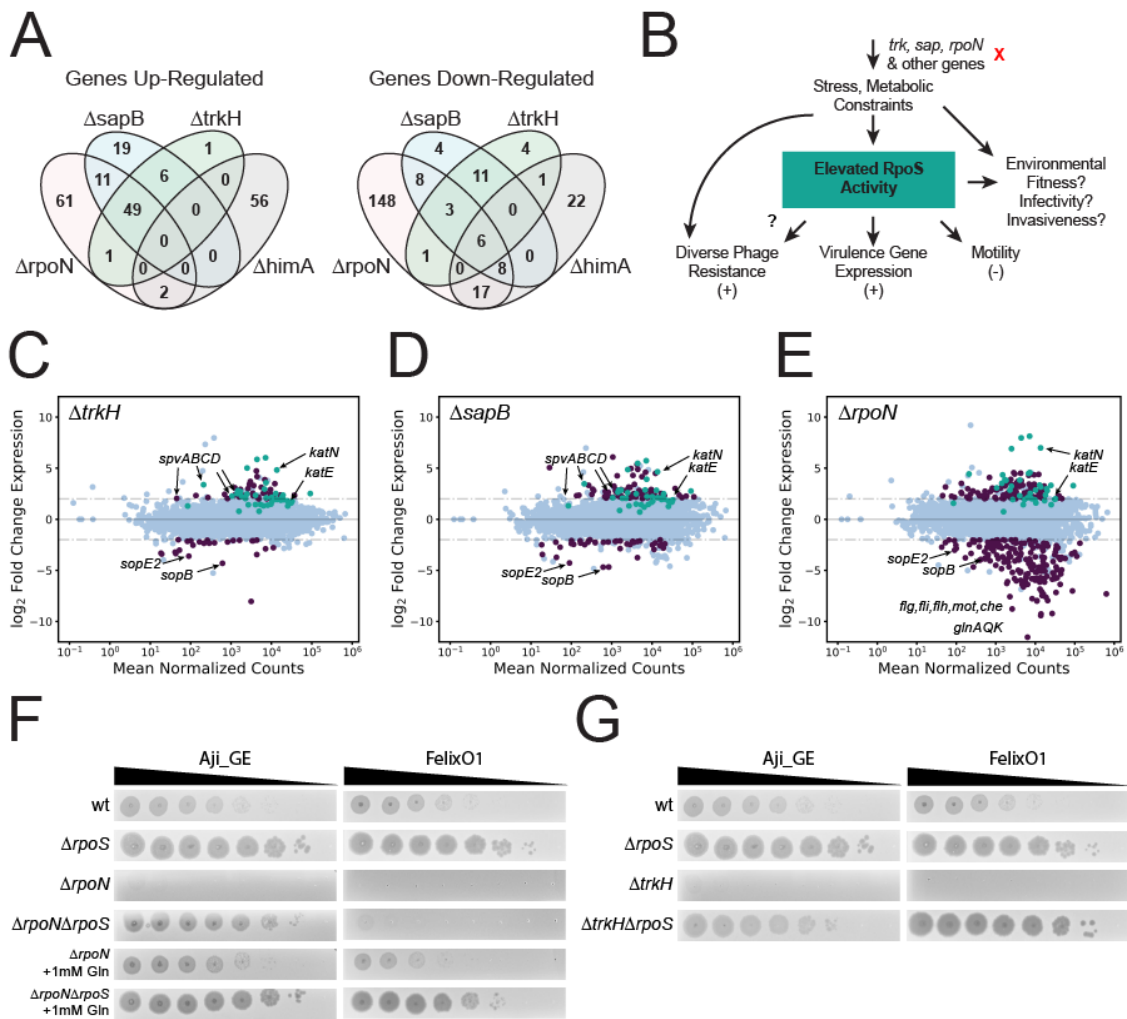
408 **Sigma Factor Interplay Mediates Phage Cross-Resistance in *Salmonella***

409 To better identify the genetic basis of the phage cross-resistance phenotype imparted by *trkH*,
 410 *sapB*, *rpoN*, and *himA* mutants, we carried out RNA-Seq experiments and investigated whole-
 411 genome expression-level differences for each deletion compared to wild-type MS1868 (N=3 for
 412 all except for *himA*, which was N=2). In aggregate, we observed 635 differentially expressed
 413 genes (among which 437 are unique to one of the knock-out strains) in *trkH*, *sapB*, *rpoN*, and
 414 *himA* mutants compared to wild-type (Figure 4A, Dataset S6). To the best of our knowledge,
 415 none of the differentially expressed genes were related to FelixO1's and Aji_GE's suspected
 416 receptors (LPS and FepA respectively). In addition, neither of the known innate immunity
 417 defense mechanisms in *S. Typhimurium* (type I CRISPR or type I BREX), were found to be
 418 differentially expressed in any of these genetic backgrounds (Barrangou and Oost, 2014;
 419 Shariat et al., 2015). Thus we suspected this mode of resistance was likely due to global
 420 regulatory changes. We focused our analysis to *trkH*, *sapB*, and *rpoN* mutant backgrounds that
 421 showed upregulation of the *spv* virulence operon (*spvABC*), located on the PSLT plasmid native
 422 to *S. Typhimurium* (Dataset S6). In addition to being studied for its essentiality in *Salmonella*
 423 virulence, the *spv* operon is also well-known for being regulated by RpoS, a general stress

424 response sigma factor (Chen et al., 1995; Fang et al., 1992; Nickerson and Curtiss, 1997). As
425 the RpoS regulation is well-studied in *E. coli* and *S. Typhimurium* (Battesti et al., 2011; Hengge-
426 Aronis, 2002; Ibanez-Ruiz et al., 2000; Lago et al., 2017; Lévi-Meyrueis et al., 2014; Lucchini et
427 al., 2009; Nickerson and Curtiss, 1997), we looked for expression changes in RpoS-dependent
428 genes in *trkH*, *sapB*, and *rpoN* mutant backgrounds. We found that a number of known RpoS-
429 regulated genes were significantly upregulated versus wild-type (passing thresholds of $\log_2FC >$
430 2 , $p_{adj} < 0.001$) (Figure 4CDE, Dataset S6), further implicating RpoS involvement in resistance
431 to both Aji_GE and FelixO1 phages (Figure 4B).

432
433 The general stress response sigma-factor RpoS activity in *Salmonella* is critical for many
434 aspects of its adaptive lifestyle, including general virulence (Lévi-Meyrueis et al., 2014; Lucchini
435 et al., 2009). However, comparative studies in clinical isolates of *Salmonella* found decreased
436 RpoS activity in model strain LT2 versus related virulent strains due to a suboptimal start codon
437 (Wilmes-Riesenberg et al., 1997). As a LT2 derivative, MS1868 has this suboptimal codon
438 (Graña et al., 1985), so it is intriguing to find signatures of elevated RpoS activity and virulence-
439 associated *spv* expression in phage resistant candidates. To confirm the impact of RpoS on
440 phage infection, we created a *rpoS* deletion mutant and additional double gene replacement
441 mutants of *rpoS* with one of *trkH*, *sapB*, or *rpoN*. The single *rpoS* deletion mutant displayed
442 increased sensitivity to both FelixO1 and Aji_GE phage (Figures 4FG and S19-S20). In addition,
443 the *rpoS* deletion was also sufficient to restore infectivity in *trkH*, *sapB*, and *rpoN* mutants to
444 levels observed in *rpoS* mutants (Figures 4FG and S19-S20). While *himA* mutants did not show
445 elevated levels of RpoS activity in our RNA-Seq data, we suspect that phage-resistance in
446 many mutants within the Aji_GE and FelixO1 cross-resistance network emerged from RpoS
447 activity beyond these mutants. More broadly, RpoS activity likely plays a role in intermediate
448 phage-resistance phenotypes that are typically difficult to quantify in pooled fitness assays, but
449 observable for these two phages.

450
451 In the *rpoN* (encoding sigma factor-54) mutant background, the *rpoS* mutation was sufficient to
452 restore infectivity of phage Aji_GE, but insufficient to restore infectivity of FelixO1 (Figures 4F
453 and S19-S20). Like RpoS, the alternate sigma factor RpoN is known to regulate a diverse set of
454 pathways involved in adaptation and survival in unfavorable environmental conditions including
455 nitrogen starvation. Because *rpoN* mutants decrease glutamine uptake and biosynthesis and
456 have significant growth defects, the phage resistance phenotype observed in *rpoN* mutants
457 potentially indicate the importance of glutamine levels on successful phage infection (Dataset
458 S4) (see also: (Aurass et al., 2018; Samuels et al., 2013)). To assess the dependence of
459 glutamine on phage resistance mechanism, we repeated phage infection supplemented with
460 glutamine in *rpoN* mutants. Both FelixO1 and Aji_GE were able to successfully plaque on *rpoN*
461 mutants supplemented with glutamine. In the *rpoN*, *rpoS* double mutant background, additional
462 glutamine supplementation was able to nearly restore FelixO1 infectivity to the *rpoS* mutant's
463 baseline (Figures 4F and S19-S20). Thus, we propose *rpoN* loss-of-function probably manifests
464 two avenues of phage resistance. First, nutrient limitation to the cell can “starve” phage
465 replication, such as FelixO1 but not Aji_GE, during infection. Second, elevated RpoS activity
466 (likely induced by nutrient limitation) confers further resistance to phage infection, extending to
467 diverse phages such as FelixO1 and Aji_GE. In summary, these studies uncover intricate
468 interplay between host factors and nutritional status of the cell in phage cross-resistance
469 phenotype.



470
 471 **Figure 4:** Cross-resistance mechanisms are mediated by RpoS. (A) Summary of genes with significant
 472 up- and down-regulation relative to wild-type for *sapB*, *trkH*, *rpoN*, and *himA* mutants. Reported values
 473 are genes with log₂-fold changes over 2 and Bonferroni-corrected p values below 0.001. (B) Proposed
 474 model for phage cross-resistance observed in this study. Loss of function of genes such as *trkH*, *sapB*, or
 475 *rpoN* impose stress and metabolic constraints on *S. Typhimurium*. In some cases, this elevates RpoS
 476 activity and leads to multi-phage resistance. However, the environmental fitness, virulence, and
 477 invasiveness implications of these mutants are not known. (CDE) MA-plots for differential expression data
 478 for (C) MS1868Δ*trkH*, (D) MS1868Δ*sapB*, and (E) MS1868Δ*rpoN* mutants over wild-type MS1868.
 479 Differentially expressed genes (abs(log₂FC ≥ 2), Bonferroni-corrected p values below 0.001) are shown in
 480 purple. RpoS-regulated genes are shown in teal based on a curated list from (Lucchini et al., 2009).
 481 Specific genes are highlighted for emphasis including RpoS-activity indicators *katE* and *katN*. (F) Aji_GE
 482 and FelixO1 phage susceptibility assays focused on Δ*rpoN*-mediated phage resistance. For both phages
 483 supplementing with glutamine (Gln) restores phage infectivity in Δ*rpoN* context. A secondary deletion in
 484 *rpoS* is sufficient to restore Aji_GE infectivity in a Δ*rpoN* strain. However, FelixO1 is only restored with

485 additional supplementation of glutamine. (G) Aji_GE and FelixO1 phage susceptibility assays focused on
486 $\Delta trkH$ -mediated phage resistance. A secondary deletion in *rpoS* is sufficient to restore both Aji_GE and
487 FelixO1 infectivity in a $\Delta trkH$ strain. Figures 4ACDE are created from Dataset S6 using Supplementary
488 Code - Figure4.

489

490 **Investigation into phage sensitivity of natural *Salmonella* strain variants**

491 Finally, we wondered how gene requirements uncovered in our genome-wide genetic screens
492 corresponded to naturally occurring variation in and phage sensitivity of *S. Typhimurium* isolates.
493 More broadly, we were interested in to what degree these gene requirements in a model strain
494 were predictive of phage sensitivity patterns in closely related strains. Though phage host range
495 determination using a panel of strains belonging to a species of bacterium is a century old
496 practice, the genetic basis of the phage infectivity pattern has remained unresolved (Holmfeldt et
497 al., 2007; Hyman and Abedon, 2010; de Jonge et al., 2019; Moller et al., 2019; Weitz et al.,
498 2013). For example, phage infectivity patterns using a panel of phages (phage typing) to
499 discriminate *Salmonella* serovars for epidemiological investigation/surveillance is even practiced
500 today, while the infectivity pattern is not typically investigated mechanistically (Chirakadze et al.,
501 2009; Rabsch, 2007). We hypothesized that the similarity and differences in genetic
502 determinants involved in phage resistance might be able to explain the genetic basis of phage
503 infectivity when extended to a panel of *Salmonella* strains. To assess the relationship between
504 genomic content and phage sensitivity among natural strain variants, we sourced a panel of 21
505 *S. Typhimurium* strains belonging to the SARA collection (Beltran et al., 1991). We also included
506 a model nontyphoid clinical isolate D23580 from Malawi (Canals et al., 2019) and ST4/74 strain,
507 originally isolated from a calf with salmonellosis (Richardson et al., 2011) as a reference. The
508 SARA collection is a set of strains of *Salmonella* isolated from a variety of hosts and
509 environmental sources in diverse geographic locations, classified into 17 electrophoretic types,
510 observed variation in natural populations and is reflective of much of the diversity identified in
511 panels derived from recent *S. Typhimurium* outbreaks (Fu et al., 2015).

512

513 We re-sequenced these 21 strains to confirm their identity and assembled their genomes as
514 described in Methods. Our analysis showed that all isolates, except for SARA7 and SARA8,
515 have a close phylogenetic relationship (>99% pairwise average nucleotide identity, ANI) in
516 agreement with an earlier report (Fu et al., 2015). Next, we searched for the 184 unique high-
517 scoring gene hits uncovered in this work (Table S4) across our panel of *Salmonella* genomes
518 and observed little variation in the sequence of genes, though there might be changes in
519 expression and activity (Dataset S8). Among the key differences in our gene content analysis,
520 we observed nonsense mutations or frame shifting changes in the coding region of *rfaK* in
521 SARA20, *ompC* and *rfbN* in SARA6 and *oafA* in SARA9 compared to our reference strain
522 *Salmonella* LT2. Mutation in the coding region of *rfaK/waaK* in SARA20 yields two truncated
523 proteins, and neither of them have a complete glycosyltransferase domain. It is known that *rfaK*
524 mutants lack the GlcNAc residue in the LPS outer core and are also unable to express O-
525 antigen because this GlcNAc residue is essential for the recognition of core oligosaccharide
526 acceptor by the O-antigen ligase WaaL (Hoare et al., 2006). We postulated that absence of outer
527 core GlcNAc (the biosynthetic product of RfaK) in SARA20 probably alters the structure of O-
528 antigen and may yield resistance to O-antigen binding by P22, SP6, Reaper_GE and FelixO1
529 phages. Disruption in the *ompC* coding region in SARA6 may compromise S16 phage infectivity
530 and disruption in *oafA* coding region (in SARA9) probably interferes with efficient infection by
531 Aji_GE. Broadly, our analysis predicts that all 23 *Salmonella* isolates except the ones mentioned

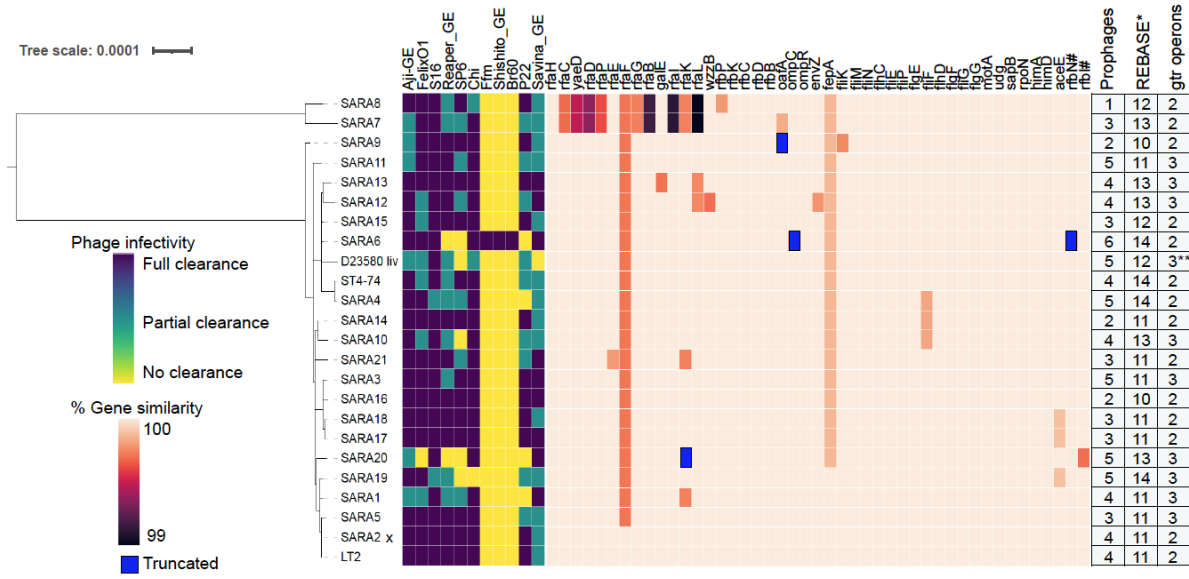
532 above should show similar phage infectivity patterns as compared to the laboratory strain used
533 in our genetic screens.

534

535 To assess the infectivity pattern of the 11 phages against the 23 *Salmonella* strains, we carried
536 out standard spotting assays. Figure 5 shows the phage infectivity data and phylogenetic
537 distance between *Salmonella* strains, with a phylogenetic tree built from gene sequences of 115
538 single-copy marker genes (Methods). In agreement with our genome-based prediction, 22
539 strains (out of 23 strains) displayed broad sensitivity to all O-antigen binding phages (except
540 Ffm, Br60 and Shashito-GE) (Figures 1-2 and 5). SARA6 was the only strain sensitive to Ffm,
541 Br60 and Shashito_GE phages and was also resistant to all phages binding O-antigen (P22,
542 SP6, Reaper_GE), indicating SARA6 may have rough-LPS phenotype. Analysis of SARA6
543 genome indicated that *rfaN*, a gene encoding rhamnosyltransferase important for O-antigen
544 synthesis has a mutation and that this strain would not be able to express O-antigen, in
545 agreement with its resistance to O-antigen binding phages (P22, SP6 and Reaper_GE) while
546 showing sensitivity to core LPS binding phages (Ffm, Br60 and Shashito-GE). Disruption of the
547 *ompC* coding region in SARA6 while retaining infectivity with S16 phage indicates there is a
548 possibility of OmpC independent infectivity pathway as seen in some T4-like phages (Washizaki
549 et al., 2016). SARA20 showed no sensitivity to both smooth-LPS binding (P22, SP6,
550 Reaper_GE, FelixO1) and rough-LPS binding phages (Ffm, Br60 and Shashito-GE), raising an
551 interesting question about its LPS architecture. Though mutation in the coding region of *rfaK*
552 and absence of O-antigen in SARA20 explains its resistance to P22, SP6, Reaper_GE, FelixO1
553 phages, though the resistance showed by rough-LPS binding phages Ffm, Br60 and Shashito-
554 GE indicate additional factors likely play a role. Finally, in agreement with our gene content
555 analysis (above), SARA9, with disruption in the *oafA* coding region, showed inefficient infection
556 by Aji_GE.

557

558 In addition to these broad agreements between gene content analysis and phage infectivity, the
559 genetic basis of strong phage resistance showed by SARA1 and SARA4 (for P22), SARA10 (for
560 SP6), D23580 (for SP6 and Savina_GE) and SARA19 (for SP6, Chi) is unclear. We also
561 observed a partial clearance pattern in our spot tests for many phages across 23 isolates,
562 probably indicating inefficient infection cycles or partial inhibition characterized by turbid
563 plaques. Overall, these results indicate that phage host range is probably defined by additional
564 constraints than the host factors uncovered in our genetic screens. To look for other host factors
565 that might be playing a role in efficient phage infection, we bioinformatically searched for
566 prophages, genes encoding O-antigen modification systems (*gtrABC* operon) and restriction
567 modification systems encoded in our panel of 23 *Salmonella* strains. The role played by these
568 genetic elements on phage infectivity and resistance are well appreciated (Bernheim and Sorek,
569 2020; Bondy-Denomy et al., 2016; Cota et al., 2015; Davies et al., 2013; Dedrick et al., 2017;
570 Dy et al., 2014; van Houte et al., 2016; Owen et al., 2020; Rostøl and Marraffini, 2019; Samson
571 et al., 2013; Vasu and Nagaraja, 2013; Wahl et al., 2019). Our comparative analysis provided a
572 list of strain-specific restriction/modification and O-antigen modification genes that may
573 influence phage infection outcome. However, we could not identify a single genomic loci, whose
574 presence or absence fully coincides with the strong phage resistance in the SARA1, SARA4,
575 SARA10, SARA19 and D23580 strains in addition to the inefficient phage infectivity pattern
576 across our panel of *Salmonella* strains. We postulate that a combination of genetic factors
577 rather than a single gene mutation probably drive the smaller changes in phage infective
578 efficiency (Datasets S8 and S9).



579
580

Figure 5. Host range of *Salmonella* phages and conservation of host factors involved in phage infection

583 Infectivity pattern of 11 phages on a panel of 23 *Salmonella* strains was inferred by spotting assay.
 584 Phylogenetic relationships of the *Salmonella* strains were estimated by phylogenetic analysis of 115
 585 single-copy marker genes (Methods). Gene similarity was calculated by TBLASTN search with LT2
 586 proteins in SARA genomes for 184 unique gene hits uncovered in this work, and 45 (out of 184) are
 587 shown in this figure (Supplementary Datasets S4 and S8) with total number of predicted prophages,
 588 restriction/modification proteins and *gtrABC* operons. Gens with premature stop codons/truncations due
 589 to insertion or deletion (compared to LT2) are marked blue. Complete detail of gene similarity of 184
 590 unique gene hits, prophages, restriction/modification proteins and *gtrABC* operons across 23 *Salmonella*
 591 strains are given in Datasets S8 and S9 * pseudogenes and incomplete genes were excluded from the
 592 analysis, SARA2 x indicates LT2 strain. ** BTP1 prophage of D23580 contains only *gtrA* and *gtrC* genes;
 593 # denotes genes that are not from the genetic screen. Figure 5 was created from Datasets S8 and S9.

594

Discussion

595
596

597 Here, we employed an unbiased RB-TnSeq loss-of-function approach to uncover the genetic
 598 determinants important in phage infection and resistance in a model enteric *Salmonella* species
 599 across 11 distinct dsDNA phages, including four phages from a therapeutic formulation. In
 600 addition to identifying known receptors for model *Salmonella* phages, our genome-wide screens
 601 identify novel receptor and non-phage-receptor host factors important for a panel of dsDNA
 602 phages. We validate many of these high fitness hits via single gene deletion strains. Our results
 603 indicate diverse modes of phage resistance including disruption in the phage infectivity pathway
 604 downstream from phage receptors. Characterization of these non-receptor phage resistance
 605 factors shared between two unrelated phages (indicating cross-resistance) identified an intricate
 606 interplay between alternative sigma factors pointing to how phage predation might be influenced
 607 by growth and nutritional status of the cell. Finally, our host-range investigation of 11 phages
 608 across a panel of 23 *Salmonella* strains showed differences in the infectivity pattern of some
 609 phages despite having high conservation of top scoring hits in our genome-wide screens in a
 610 closely related model organism. Comparative analysis identified instances where sequence

611 variation in target receptor explained some of the phage susceptibility pattern, but there are
612 additional factors and interactions both in the target host and phages that defines the host
613 range. Overall this study highlights the importance of unbiased high-throughput genetic screens
614 across a panel of phages in uncovering diversity of host factors important phage infection,
615 provides insights on the genetic basis and modes of cross-resistance between sets of phages,
616 and uncover gaps in our understanding of phage host-range across natural bacterial isolates.

617
618 Our genome-wide screens also suggest how phage selection can be used to drive beneficial
619 tradeoffs to modulate pathogen virulence, sensitivity and fitness. For example, LPS and O-
620 antigen play a critical role in the lifestyle of *Salmonella* virulence and have a myriad of effects on
621 phage predation. Phage selection to drive truncation, loss, or reduction of LPS and O-antigen in
622 *Salmonella* could be employed to decrease virulence and increase its susceptibility to
623 antibiotics, decreased swarming motility, decreased colonization, and decreased fitness (Kong
624 et al., 2011; Nagy et al., 2006; Toguchi et al., 2000). Our investigation into a network of cross-
625 resistant genotypes against unrelated phages FelixO1 and Aji_GE led to the role of RpoS and
626 RpoN activity, a virulence-regulating alternative sigma factors in *Salmonella* sp (Chen et al.,
627 1995; Fang et al., 1992; Wilmes-Riesenberg et al., 1997) on phage infectivity. Specifically, the
628 association of increased RpoS activity with phage resistance raises intriguing ecological
629 questions for consideration. While RpoS activity is associated with virulence, are these phage-
630 resistant genotypes more virulent and fit in infection contexts? Further, do these genotypes
631 display increased RpoS activity and/or virulence in more virulent *Salmonella* strains? If so, the
632 selection for increased phage-resistant strains with increased virulence-associated RpoS
633 activity would be a deleterious outcome from therapeutic phage predation and an undesirable
634 criterion for potentially therapeutic phages. Conversely, does the lack of phage predation
635 contribute to the neutral drift of RpoS alleles and virulence in laboratory settings (Robbe-Saule
636 et al., 1995; Wilmes-Riesenberg et al., 1997)? It is known that RpoS directly and indirectly
637 regulates more than 10% of all genes in *E. coli* (Battesti et al., 2011) and *S. Typhimurium* (Lago
638 et al., 2017; Lévi-Meyrueis et al., 2014), and is involved in adaptation to diverse environments
639 and metabolic states (Battesti et al., 2011, 2015; Hengge-Aronis, 2002; Lucchini et al., 2009;
640 Nickerson and Curtiss, 1997; Robbe-Saule et al., 1995). Thus, phage resistance phenotypes
641 associated with RpoS activity may be acting through activation of RpoS-mediated stress
642 response pathways rather than the direct loss of RpoS itself. In some cases, dual regulation by
643 genetic or nutritional factors and RpoS could lead to compensation. Some of these genotypes
644 (for example, mutants in *trk*, *sap*, *ace*, and *rpoN*) were recently associated with phage resistance
645 in *E. coli* (Cowley et al., 2018; Kortright et al., 2020) and *P. aeruginosa* (Wright et al., 2018), but
646 are not yet linked to RpoS activity. Future work will explore if we see similar dependencies of
647 alternative sigma-factors on phage resistance phenotypes in other pathogens (Dong and
648 Schellhorn, 2010).

649
650 Our investigation into the host-range of *Salmonella* phages across closely related *Salmonella*
651 isolates indicated that the highly fit phage resistance genotypes uncovered via genome-wide
652 genetic screens are not complete predictors of phage infectivity and host range. Though these
653 host factors showed little variation in their sequences across our panel of *Salmonella* isolates, it
654 is possible that they vary in expression and activity, sufficient to impact phage infectivity cycle.
655 The host-range of phages is not only defined by whether the host is susceptible to phage
656 infection, but also on how phages evade host defences and overcome barriers to efficient
657 infection. For example, Because O-antigen structures in *Salmonella typhimurium* sp. can
658 comprise over 400 sugars per O-antigen LPS molecule (Crawford et al., 2012), it is no surprise
659 that many bacteriophages adsorb to this highly exposed structure. However, many

660 bacteriophages that adsorb to centralized outer membrane receptors can be occluded from their
661 native receptor by the O-antigen structure (Domínguez-Medina et al., 2020). Systematic studies
662 exploring the form and structure of O-antigens and how they impact accessibility of phage
663 receptors are needed. We postulate that there are likely additional constraints affecting optimal
664 phage infectivity, and probably we might have missed uncovering these additional factors in our
665 model strain because of highly fit phage receptor mutants. Considering differences in phage
666 infectivity in a panel of strains with highly conserved genetic determinants, we posit that
667 systematic study of differences in transcriptional and translation processes in these strains
668 might provide more insights as illustrated in a few recent phage-host interaction
669 studies (Brandão et al., 2021; Howard-Varona et al., 2018). Future studies could also employ
670 recently developed methods (Mutalik et al., 2019; Rishi et al., 2020; Thibault et al., 2019) to
671 provide higher resolution into phage-host interactions and may aid in filling the knowledge gaps
672 on phage host-range. These methods could be extended to a few closely related and
673 phylogenetically distant strains to understand the variability in host factors impacting phage
674 infectivity patterns. Finally, by combining the genetic tools developed for functional assessment
675 of host genes with targeted or genome-wide loss-of-function mutant libraries in few model
676 phages, can provide additional insights into the host specificity of phages.

677
678 As high-throughput genetic screens to understand phage-host interactions grow more
679 commonplace across diverse bacteria (Bohm et al., 2018; Christen et al., 2016; Cowley et al.,
680 2018; Mutalik et al., 2019; Pickard et al., 2013; Price et al., 2018; Rishi et al., 2020; Rousset et
681 al., 2018; Wetmore et al., 2015), leveraging fitness data across phages and bacterial genetic
682 diversity constitutes a major challenge and opportunity. Further screens against antibiotics, such
683 as those presented in earlier (Price et al., 2018), could rapidly discover collateral sensitivity
684 patterns wherein phage resistant genotypes display sensitization to antibiotics or ecologically-
685 relevant conditions (for instance sera or bile salts). Such information has the potential to form
686 the basis of successful combinations of treatments (Chan et al., 2018; Kortright et al., 2019;
687 Mangalea and Duerkop, 2020). We posit that phage-host interaction studies across diverse
688 bacterial isolates in a range of biotic and abiotic conditions powered with novel transcriptomics
689 and proteomics tools can provide rich datasets for host-range predictive models and rational
690 phage cocktails formulations.

691
692

693 **Materials and Methods**

694

695 **Bacterial strains and growth conditions**

696 Strains, primers, and plasmids are listed in Tables S3-S5, respectively. *S. Typhimurium* LT2
697 derivative strain MS1868 genotype is *S. Typhimurium* LT2 (leuA414(Am) Fels2- hsdSB(r-
698 m+))(Graña et al., 1985). In general, all *Salmonella* strains were grown in Luria-Bertani (LB-
699 Lennox) broth (Sigma) at 37°C, 180 rpm unless stated otherwise. When appropriate, 50 µg/mL
700 kanamycin sulfate and/or 34 µg/mL chloramphenicol were supplemented to media. For strains
701 containing an ampR selection marker, carbenicillin was employed at 100 µg/mL, but exclusively
702 used during isolation of clonal mutants to avoid mucoidy phenotypes. All bacterial strains were
703 stored at -80°C for long term storage in 25% sterile glycerol (Sigma).

704

705 **Bacteriophages and propagation**

706 Bacteriophages employed in this study and sources are listed in Table 1. All phages were either
707 successively serially diluted or streaked onto 0.7% LB-agar overlays for isolation. For
708 bacteriophage Chi, 0.35% LB-agar overlays were employed. Bacteriophage Aji_GE_EIP16,
709 Reaper_GE_8C2, Savina_GE_6H2, and Shishito_GE_6F2 were isolated from a commercial
710 bacteriophage formulation from Georgia. All phages isolated from this source are denoted with
711 “_GE” (to recognize being sourced from Georgia). All other bacteriophages were re-isolated
712 from lysates provided from stock centers or gifts from other labs (Table 1). Bacteriophage
713 Aji_GE_EIP16, Chi, FelixO1, P22 (a strictly lytic mutant), Reaper_GE_8C2, S16, and SP6 were
714 isolated and scaled on *S. Typhimurium* MS1868. Bacteriophage Br60, Ffm, Savina_GE_6H2,
715 and Shishito_GE_6F2 were isolated and rough-LPS mutant *S. Typhimurium*. SL733 (BA1256).
716 We followed standard protocols for propagating phages (Kutter and Sulakvelidze, 2004). Br60,
717 Chi, Ffm, P22, Reaper_GE_8C2, S16, Savina_GE_6H2, Shishito_GE_6F2, and SP6 were
718 propagated in LB-Lennox liquid culture on their respective strains. Reaper_GE_8C2,
719 Savina_GE_6H2, and Shishito_GE_6F2 were additionally buffer-exchanged into SM-Buffer
720 (Teknova) via ultrafiltration (Amicron 15) and resuspension. Bacteriophage Aji_GE_EIP16 and
721 FelixO1 were propagated in LB-Lennox liquid culture on their respective strains and further
722 propagated through a standard overlay method. Whenever applicable, we used SM buffer
723 without added salts (Tekova) as a phage resuspension or dilution buffer and routinely stored
724 phages as filter-sterilized (0.22µm) lysates at 4°C.

725

726 Bacteriophages Aji_GE_EIP16, Reaper_GE_8C2, Savina_GE_6H2, and Shishito_GE_6F2
727 were additionally whole-genome sequenced and assembled. Approximately 1e9 PFU of phage
728 lysate was gDNA extracted through Phage DNA Isolation Kit (Norgen, 46800) as per
729 manufacturer's instructions. Library preparation was performed by the Functional Genomics
730 Laboratory (FGL), a QB3-Berkeley Core Research Facility at UC Berkeley. Sequencing was
731 performed at the Vincent Coates Sequencing Center, a QB3-Berkeley Core Research Facility at
732 UC Berkeley on a MiSeq using 75PE runs for Reaper_GE_8C2, Savina_GE_6H2, and
733 Shishito_GE_6F2 and using 150SR run for Aji_GE_EIP16. Phage genomes were assembled
734 using KBase (Arkin et al., 2018). Illumina reads were trimmed using Trimmomatic v0.36 (Bolger
735 et al., 2014) and assessed for quality using FASTQC. Trimmed reads for Aji_GE_EIP16,
736 Reaper_GE_8C2, and Shishito_GE_6F2 were assembled using Spades v3.13.0 (Nurk et al.,
737 2013). Trimmed reads for Savina_GE_6H2 were assembled using Velvet v1.2.10 (Zerbino and
738 Birney, 2008). The primary, high coverage contig from these assemblies was investigated and
739 corrected for incorrect terminus assembly using PhageTerm v1.011 on CPT Galaxy (Garneau et
740 al., 2017). In this manuscript, we limited analyses of these sequences to assessing phylogeny of
741 these phages, which we performed with BLASTN (Dataset S7). A detailed genomic

742 characterization will be published by Dr. Elizabeth Kutter. Sequences and preliminary
743 annotations can be found at JGI IMG under analysis projects Ga0451357, Ga0451371,
744 Ga0451358, and Ga0451372.

745

746 **Construction of MS1868 RB-TnSeq library**

747 We created the *Salmonella enterica* serovar Typhimurium MS1868 (MS1868_ML3) transposon
748 mutant library by conjugating with *E. coli* WM3064 harboring pHLL250 mariner transposon
749 vector library (strain AMD290) (Figure S1). To construct pHLL250, we used the magic pools
750 approach we outlined previously (Liu et al., 2018). Briefly, pHLL250 was assembled via Golden
751 Gate assembly using BbsI from part vectors pHLL213, pHLL216, pHLL238, pHLL215, and
752 pJW14 (Liu et al., 2018). We then incorporated millions of DNA barcodes into pHLL250 with a
753 second round of Golden Gate assembly using BsmBI. Briefly, we grew *S. Typhimurium* LT2
754 MS1868 at 30°C to mid-log-phase and combined equal cell numbers of *S. Typhimurium* LT2
755 MS1868 and donor strain AMD290, conjugated them for 5 hrs at 30°C on 0.45- μ m nitrocellulose
756 filters (Millipore) overlaid on LB agar plates containing diaminopimelic acid (DAP) (Sigma). The
757 conjugation mixture was then resuspended in LB and plated on LB agar plates with 50 μ g/ml
758 kanamycin to select for mutants. After 1 day of growth at 30°C, we scraped the kanamycin-
759 resistant colonies into 25 mL LB and processed them as detailed earlier to make multiple 1-mL -
760 80°C freezer stocks. To link random DNA barcodes to transposon insertion sites, we isolated
761 the genomic DNA from cell pellets of the mutant libraries with the DNeasy kit (Qiagen) and
762 followed published protocol to generate Illumina compatible sequencing libraries (Wetmore et al.,
763 2015). We then performed single-end sequencing (150 bp) with the HiSeq 2500 system
764 (Illumina). Mapping the transposon insertion locations and the identification of their associated
765 DNA barcodes was performed as described previously (Price et al., 2018). In total, our 66,996
766 member pooled library consisted of transposon-mediated disruptions in 3,759 out of 4,610
767 genes, with an average of 14.8 disruptions per gene (median 12). Compared to a non-barcoded
768 reported transposon mutant library in *S. Typhimurium* 14028s (Porwollik et al., 2014), we
769 suspect 434 of the 851 unmutated genes are likely essential, and 380 likely nonessential. We
770 abstain from interpreting essentiality of 37 additional genes due to inability to uniquely map
771 insertions or due to gene content differences between the two libraries. Additional details for the
772 composition of the *S. Typhimurium* MS1868 library can be found in Table S1 and Dataset S1.

773

774 **Liquid culture “competitive” fitness experiments**

775 Competitive, phage-stress fitness experiments were performed in liquid culture, as phage
776 progeny from an infection of one genotype could subsequently infect other host genotypes. All
777 bacteriophages were tested against the MS1868 library. Bacteriophage Br60, Ffm, and
778 Shishito_GE_6F2 were additionally tested against the previously described *E. coli* BW25113
779 library (Wetmore et al., 2015). To avoid jackpot effects, at least two replicate experiments were
780 performed per phage-host library experiment as presented earlier (Mutalik et al., 2020). Briefly,
781 a 1 mL aliquot of RB-TnSeq library was gently thawed and used to inoculate a 25 mL of LB
782 supplemented with kanamycin. The library culture was allowed to grow to an OD600 of ~1.0 at
783 37°C. From this culture we collected three, 1 mL pellets, comprising the ‘Time-0’ or reference
784 samples in BarSeq analysis. The remaining cells were diluted to a starting OD600 of 0.04 in 2X
785 LB with kanamycin. 350 μ L of cells were mixed with 350 μ L phage diluted in SM buffer to a
786 predetermined MOI and transferred to a 48-well microplate (700 μ L per well) (Greiner Bio-One
787 #677102) covered with breathable film (Breathe-Easy). Phage infection progressed in Tecan
788 Infinite F200 readers with orbital shaking and OD600 readings every 15 min for 3 hours at 37°C.
789 At the end of the experiment, each well was collected as a pellet individually. All pellets were
790 stored at -80°C until prepared for BarSeq.

791

792 **Solid agar “noncompetitive” fitness experiments**

793 Noncompetitive, phage-stress fitness experiments were performed on solid-agar plate culture as
794 presented earlier (Mutalik et al., 2020). Solid plate fitness experiments were performed by
795 assaying all 11 bacteriophages against the MS1868 library. Bacteriophage Br60, Ffm, and
796 Shishito_GE_6F2 were additionally assayed on the *E. coli* BW25113 library (Wetmore et al.,
797 2015). For the solid plate experiments a 1 mL aliquot of the RB-TnSeq library was gently
798 thawed and used to inoculate a 25 mL LB supplemented with kanamycin. The library culture
799 was allowed to grow to an OD600 of ~1.0 at 37°C. From this culture we collected three, 1 mL
800 pellets, comprising the ‘Time-0’ for data processing in BarSeq analysis. The remaining cells
801 were diluted to a starting OD600 of 0.01 in LB with kanamycin. 75 µL of cells were mixed with
802 75 µL of phage diluted in SM buffer to a predetermined MOI and allowed to adsorb for 10
803 minutes. The entire culture was spread evenly over a LB agar plate with kanamycin and grown
804 overnight at 37°C. The next day, all resistant colonies were collected and suspended in 1.5 mL
805 LB media before pelleting. All pellets were then stored at -80°C until prepared for BarSeq.

806

807 **BarSeq of RB-TnSeq pooled fitness assay samples**

808 Genomic DNA was isolated from stored pellets of enriched and ‘Time 0’ RB-TnSeq samples
809 using the DNeasy Blood and Tissue kit (Qiagen). We performed 98°C BarSeq PCR protocol as
810 described previously (Mutalik et al., 2020; Wetmore et al., 2015). BarSeq PCR in a 50 µL total
811 volume consisted of 20 µmol of each primer and 150 to 200 ng of template genomic DNA. For
812 the HiSeq4000 runs, we used an equimolar mixture of four common P1 oligos for BarSeq, with
813 variable lengths of random bases at the start of the sequencing reactions (2–5 nucleotides).
814 Equal volumes (5 µL) of the individual BarSeq PCRs were pooled, and 50 µL of the pooled PCR
815 product was purified with the DNA Clean and Concentrator kit (Zymo Research). The final
816 BarSeq library was eluted in 40 µL water. The BarSeq samples were sequenced on Illumina
817 HiSeq4000 instruments with 50 SE runs. Typically, 96 BarSeq samples were sequenced per
818 lane of HiSeq.

819

820 **Data processing and analysis of BarSeq reads**

821 Fitness data for the RB-TnSeq library was analyzed as previously described (Wetmore et al.,
822 2015). Briefly, the fitness value of each strain (an individual transposon mutant) is the
823 normalized $\log_2(\text{strain barcode abundance at end of experiment} / \text{strain barcode abundance at}$
824 $\text{start of experiment})$. The fitness value of each gene is the weighted average of the fitness of its
825 strains. Further analysis of BarSeq data was carried out in Python3 and visualized employing
826 matplotlib and seaborn packages. For heatmap visualizations, genes with under 25 BarSeq
827 reads in the phage samples had their fitness values manually set to 0 to avoid artificially high
828 fitness scores (due to the strong selection pressure imposed by phage predation).

829

830 Due to the strong selection pressure and subsequent fitness distribution skew resulting from
831 phage infection, a couple additional heuristics were employed during analysis. Initially, per
832 phage experiment, fitness scores were filtered for \log_2 -fold-change thresholds, aggregated read
833 counts, and t-like-statistics. Experiments using phages Ffm, Shishito_GE, and Br60 (which
834 cannot infect wild-type MS1868, but can infect specific MS1868 mutants) against the MS1868
835 library employed negative thresholds to identify sensitized genotypes. A summary of \log_2 -fold-
836 change fitness and t-like statistic thresholds are provided in the Dataset S2. Each reported hit
837 per phage was further processed via manual curation to minimize reporting of false-positive
838 results due to the strong phage selection pressure. Here, all individual barcodes per genotype
839 were investigated simultaneously for each experiment through both barcode-level fitness scores

840 and raw read counts. First, genotypes were analyzed for likely polar effects. If the location and
841 orientation of each fit barcode were exclusively against the orientation of transcription and/or
842 exhibited strong fitness at the C-terminus of a gene, while being transcriptionally upstream of
843 another fit gene, the genotype was likely a polar effect and eliminated. Second, genotypes were
844 analyzed for jackpot fitness effects that could indicate a secondary site mutation. These cases
845 were identified by investigating consistency between individual strains within a genotype. If the
846 vast majority of reads per genotype belonged to a singular mutant (of multiple), we attributed the
847 aggregate fitness score to secondary-site mutation effects and eliminated those genotypes from
848 reported results. Genotypes where there were too few strains to make a judgment call on within
849 genotype strain consistency (ie 1-3 barcodes) were generally excluded from analysis unless
850 they were genotypes consistent with other high-scoring genotypes. Next, we investigated for
851 consistency between read counts and fitness scores at both the strain level. In general, we
852 found that strains with read counts under 25 often had inflated fitness scores under strong
853 phage selection pressure and the subsequent fitness distribution skew resulting from phage
854 infection. Cases where high fitness scores were attributed to a couple of strains with reads
855 under 25 were eliminated as false positives as well. Finally, all genotypes were loosely curated
856 for consistency across liquid experiments. Cases that barely passed confidence thresholds as
857 described above that were inconsistent across replicate experiments were eliminated from
858 reporting. A summary of fit genotypes that passed automated filtering and manual curation are
859 reported in Dataset S4. No fit genotypes were added during manual analyses.

860
861 Network graphs were constructed using Gephi. Graph layout optimization was determined
862 through a combination of manual placement of nodes (for instance phage nodes in Figure 3B)
863 and layout optimization based off of equally weighted edges using the Yifan Hu algorithm. In all
864 graphs, edges were calculated based on Dataset S4 using custom python scripts. In brief, in the
865 mixed node graph in Figure 3B, edges were drawn with weight 1 between a phage node (fixed)
866 and a gene node if that gene conferred resistance according to Dataset S4.

867
868 **Individual Mutant Creation**
869 All individual deletion mutants in *S. Typhimurium* were created through lambda-red mediated
870 genetic replacement (Sawitzke et al., 2007). Per deletion, primers were designed to PCR
871 amplify either kanamycin or ampicillin selection markers with ~30-40 bp of homology upstream
872 and downstream of the targeted gene locus, leaving the native start and stop codons intact
873 preserving directionality of gene expression at the native locus (Table S3). PCRs were
874 generated and gel-purified through standard molecular biology techniques and stored at -20°C
875 until use. All strains (including mutants) employed in this study are listed in Table S5.

876
877 Deletions were performed by incorporating the above dsDNA template into the *Salmonella*
878 genome through standard pSIM5-mediated recombineering methods (Sawitzke et al., 2007).
879 First temperature-sensitive recombineering vector, pSIM5, was introduced into the relevant
880 *Salmonella* strain through standard electroporation protocols and grown with chloramphenicol at
881 30°C. Recombination was performed through electroporation with an adapted pSIM5
882 recombineering protocol. Post-recombination, clonal isolates were streaked onto plates without
883 chloramphenicol at 37°C to cure the strain of pSIM5 vector, outgrown at 37°C and stored at -
884 80°C until use. For double deletions, this process was repeated two times in series with
885 kanamycin followed by ampicillin selection markers. Gene replacements were verified by colony
886 PCR followed by Sanger sequencing at the targeted locus (both loci if a double deletion mutant)
887 and 16S rDNA regions (primers provided in Table S3).

888

889 **Assessing Phage Sensitivity**

890 Phage-resistance and -sensitivity was assessed through efficiency of plating experiments.
891 Bacterial hosts were grown overnight at 37°C. 100 µL of these overnight cultures were added to
892 5 mL of top-agar with appropriate antibiotics and allowed to solidify at room temperature. For
893 assays including supplements such as glutamine, the supplement was added directly to the top
894 agar layer. Phages were ten-fold serially diluted in SM Buffer, two microliters spotted out on the
895 solidified lawn, and incubated the plates overnight at 37°C. Efficiency of plating was calculated
896 as the ratio of the average effective titer on the tested host to the titer on the propagation host.
897 For some assay strains, plaques showed diffused morphology and were difficult to count, or
898 displayed plaque phenotypes distinct from its propagation host. In all cases, representative
899 images are presented (Figures S5-S11, S13-S15). All plaquing experiments were performed
900 with at least three biological replicates, each replicate occurring on a different day from a
901 different overnight host culture.
902

903 **RNA-Seq experiments**

904 Samples for RNA-Seq analysis were collected and analyzed for wild-type MS1868 (BA948)
905 (N=3), knockout mutants for *trkH* (BA1124) (N=3) *sapB* (BA1136) (N=3), *rpoN* (BA1139) (N=3),
906 and *himA* (BA1142) (N=2). All cultures for RNA-Seq were grown on the same day from unique
907 overnights and subsequent outgrowths. Strains were diluted to OD600 ~0.02 in 10 mL LB with
908 appropriate selection marker, and then grown at 30°C at 180 RPM until they reached an OD600
909 0.4-0.6. Samples were collected as follows: 400 µL of culture was added to 800 µL RNAProtect
910 (Qiagen), incubated for 5 minutes at room temperature, and centrifuged for 10 minutes at
911 5000xg. RNA was purified using RNeasy RNA isolation kit (Qiagen) and quantified and quality-
912 assessed by Bioanalyzer. Library preparation was performed by the Functional Genomics
913 Laboratory (FGL), a QB3-Berkeley Core Research Facility at UC Berkeley. Illumina Ribo-Zero
914 rRNA Removal Kits were used to deplete ribosomal RNA. Subsequent library preparation steps
915 of fragmentation, adapter ligation and cDNA synthesis were performed on the depleted RNA
916 using the KAPA RNA HyperPrep kit (KK8540). Truncated universal stub adapters were used for
917 ligation, and indexed primers were used during PCR amplification to complete the adapters and
918 to enrich the libraries for adapter-ligated fragments. Samples were checked for quality on an
919 Agilent Fragment Analyzer, but ribosome integrity numbers were ignored. This is routine for
920 *Salmonella* sp., since they natively have spliced 23S rRNA (Burgin et al., 1990). Sequencing
921 was performed at the Vincent Coates Sequencing Center, a QB3-Berkeley Core Research
922 Facility at UC Berkeley on a HiSeq4000 using 100PE runs.
923

924 **RNA-Seq Data Analysis**

925 For all RNA-Seq experiments, analyses were performed through a combination of KBase-(Arkin
926 et al., 2018) and custom jupyter notebook-based methods. The data processing narrative in
927 KBase can be found here: <https://kbase.us/n/48675/70/>. StringTie and DESeq2 KBase outputs
928 are currently available in Datasets S5 and S6 (<https://doi.org/10.6084/m9.figshare.12185031>).
929 Briefly, Illumina reads were trimmed using Trimmomatic v0.36 (Bolger et al., 2014) and
930 assessed for quality using FASTQC. Trimmed reads were subsequently mapped to the *S.*
931 *Typhimurium* LT2 along with PSLT genome (NCBI Accession: AE006468.2 and AE006471.2
932 respectively) with HISAT2 v2.1.0 (Kim et al., 2019). Alignments were quality-assessed with
933 BAMQC. From these alignments, transcripts were assembled and abundance-estimated with
934 StringTie v1.3.3b (Pertea et al., 2015). Tests for differential expression were performed on
935 normalized gene counts by DESeq2 (negative binomial generalized linear model) (Love et al.,
936 2014). Additional analyses for all experiments were performed in Python3 and visualized
937 employing matplotlib and seaborn packages. Conservative thresholds were employed for

938 assessing differentially expressed genes. Conclusions were considered differentially expressed
939 if they possessed a Bonferoni-corrected p-value below a threshold of 0.001 and an absolute
940 log₂ fold change greater than 2. Assembled transcripts from StringTie and differential
941 expression from RNA-Seq analyses can be found in Datasets S5 and S6 respectively.

942

943 **Genome sequencing of SARA collection**

944 We sequenced the 21 reference *S. Typhimurium* genomes(Beltran et al., 1991)using standard
945 molecular biology protocols. Briefly, we grew up all 21 strains to stationary phase in LB media.
946 We then extracted gDNA using the DNeasy Blood and Tissue kit (Qiagen). Illumina library
947 preparation was performed by the Functional Genomics Laboratory (FGL), a QB3-Berkeley
948 Core Research Facility at UC Berkeley. Sequencing was performed at the Vincent Coates
949 Sequencing Center, a QB3-Berkeley Core Research Facility at UC Berkeley on a HiSeq4000
950 using 100PE reads. We used Unicycler with default parameters(Wick et al., 2017) to do a
951 reference based assembly from closely related *Salmonella* strains.

952 **Bioinformatic analysis of SARA collection genomes**

953 Predicted genes in 24 *Salmonella typhimurium* genomes were classified in families of
954 homologous genes by PPanGGoliN(Gautreau et al., 2020). Gene clusters encoding LPS core
955 oligosaccharide and O-specific antigen (OSA) biosynthetic enzymes were identified in the
956 *Salmonella* genomes by search for gene families containing characterized LPS and OSA
957 biosynthesis genes of LT2 strain (STM2079-STM2098, STM3710-STM3723)(Heinrichs et al.,
958 1998; Seif et al., 2019). O-antigen modification genes were identified by DIAMOND similarity
959 search(Buchfink et al., 2015) with characterized LT2 proteins OpvA (STM2209), OpvB
960 (STM2208), GtrA (STM0559, STM4204), GtrB(STM0558, STM4205)(Broadbent et al., 2010)
961 using blastp command with --very-sensitive option. Restriction/modification genes were
962 identified by DIAMOND similarity search with 78008 proteins from REBASE database(Roberts
963 et al., 2015). Point mutations in LPS and OSA biosynthesis enzymes were identified by running
964 a command-line application for TBLASTN search(Camacho et al., 2009) of LT2 proteins vs.
965 genome sequences of 23 *Salmonella typhimurium* genomes.

966 **Phylogenetic analysis**

967 To estimate phylogenetic relationships between genomes of our collection of *Pseudomonas*
968 spp. strains, we identified a set of 120 bacterial marker genes with GTDB-Tk toolkit(Chaumeil et
969 al., 2019). Only 115 marker genes were found in single copy in each of the 24 genomes studied.
970 Gene sequences of those 115 markers were aligned by MAFFT v7.310(Katoh and Standley,
971 2014) with --auto option, and the resulting 88 alignments were concatenated into a single
972 multiple sequence alignment. A phylogenetic tree was reconstructed from the multiple alignment
973 using the maximum likelihood method and generalized time-reversible model of nucleotide
974 substitution implemented in the FastTree software v2.1.10(Price et al., 2010) and visualized
975 using the Interactive Tree of Life (iTOL) online tool(Letunic and Bork, 2019).

976

977 **Prophage analysis**

978 To determine prophage content, we submitted all contigs longer than 10kb to the PHASTER
979 web server, culminating in 250 potential prophage regions across the 21 strains
980 investigated(Arndt et al., 2016) (Dataset S9). These 250 identified regions were aligned against
981 each other using nucmer(Marçais et al., 2018). Grouping and subsequent filtering of prophages
982 was performed through network graph analysis using Gephi; prophage nodes were connected
983 by edges representing total nucmer alignments greater than 60% alignment. Graph layout
984 optimization was determined through layout optimization based off of equally weighted edges

985 using the Yifan Hu algorithm. For each “cluster” of prophages and each alone prophage, a few
986 representatives were investigated manually for prophage similarity to determine if a PHASTER-
987 identified region (or “cluster”) was correctly identified as a prophage, yielding 84 likely prophage
988 regions. Based on similarity to studied prophages, we assigned each “cluster” to one of “ST64B
989 (118970_sal3-like)”, “Gifsy-1”, “Gifsy-2”, “Gifsy-3”, “Fels-1”, “P2-like”, “P22-like”, “phiKO2-like”,
990 “SPN1S-like” classifications (Dataset S9).

991
992 Because this prophage determination was based upon a reference-based assembly(Wick et al.,
993 2017), it was possible for some regions to mis-assemble depending on the reference genome
994 used. So, we further validated if these prophage regions were artifacts of assembly. For each
995 genome, we re-aligned our reads to the assembled genome using samtools and noted all
996 regions that were not covered in BAM-alignments. We noted if prophages were either (1) split
997 across contigs (common for “Gifsy-2”), (2) not covered by reads (noted 2 instances for P22-like
998 prophages), (3) partially not covered by reads (common for P22-like phages, which have known
999 mosaic sequences)(Fu et al., 2017) and (4) compared our prophage identification efforts to
1000 earlier work(Fu et al., 2017). After eliminating prophage regions that were assembly artifacts, we
1001 culminated in 74 high confidence prophage regions across the 21 SARA strains (Dataset S9).

1002
1003 **Acknowledgments**
1004 The authors gratefully thank Kenneth Sanderson (*Salmonella* Genetic Stock Center), Michael
1005 McClelland, Sylvain Moineau (Félix d'Hérelle Reference Center for Bacterial Viruses), Richard
1006 Calendar, Ian J. Molineux, and Jason J. Gill for sharing bacterial strains and phages and
1007 supplying valuable advice. Additionally, we would like to thank Morgan Price for helpful
1008 conversations during analysis and preparation of the manuscript.

1009 This project was funded by the Microbiology Program of the Innovative Genomics Institute,
1010 Berkeley. The initial concepts for this project were funded by ENIGMA, a Scientific Focus Area
1011 Program at Lawrence Berkeley National Laboratory, supported by the U.S. Department of
1012 Energy, Office of Science, Office of Biological and Environmental Research under contract DE-
1013 AC02-05CH11231.

1014 RNA sample processing and library creation was performed at Functional Genomics Lab,
1015 Vincent J. Coates Genomics Sequencing Lab, & Computational Genomics Resources Lab
1016 (University of California at Berkeley). Sequencing was performed at: Vincent J. Coates
1017 Genomics Sequencing Laboratory (University of California at Berkeley), supported by NIH S10
1018 Instrumentation Grants S10RR029668, S10RR027303, and OD018174.

1019
1020 **Author Contributions**
1021 B.A.A., V.K.M., and A.P.A. conceived the project.
1022 B.A.A. led the experimental work, analysis, and manuscript preparation.
1023 B.A.A., V.K.M., C.Z., A.M.D. and H.L. built and characterized the RB-TnSeq library.
1024 B.A.A. performed experiments, processed, and analyzed data.
1025 E.B.K. provided critical reagents and advice.
1026 T.N.N., L.M.L. assembled genomes.
1027 B.A.A., E.B.K., A.M.D., V.K.M., and A.P.A. wrote the paper.

1028
1029 **Competing Interests**
1030 V.K.M., A.M.D., and A.P.A. consult for and hold equity in Felix Biotechnology Inc..

1031
1032
1033

1034 **Data Availability**

1035 Supplementary Information can be found here:

1036 <https://doi.org/10.6084/m9.figshare.12185001.v2>. Complete Supplementary Datasets can be
1037 found here: <https://doi.org/10.6084/m9.figshare.12185031>. Supplementary Code and figure
1038 reproduction can be found here: <https://doi.org/10.6084/m9.figshare.12412814.v2>. All NGS
1039 reads have been deposited and made publicly accessible via the Sequence Read Archive
1040 (SRA) under Bioproject PRJNA638761: <http://www.ncbi.nlm.nih.gov/bioproject/638761>. Draft
1041 *S.Typhimurium* genome sequences for strains SARA1-SARA21 can be found under
1042 BioSamples SAMN17506935-SAMN17506955. Draft phage genome sequences and JGI-
1043 performed gene annotations can be found at JGI IMG under analysis projects Ga0451357,
1044 Ga0451371, Ga0451358, and Ga0451372. The RNA-Seq data processing narrative in KBase
1045 can be found here: <https://kbase.us/n/48675/70/>.

1046 *Table 1. Bacteriophages employed in this study.*
 1047 Virus families were assigned via ICTV taxonomy release 2019. For new phages isolated in this
 1048 study, the family of the nearest BLASTN relative was reported (in line with ICTV 2019
 1049 standards). This information can be found in Dataset S7.

Phage	Family	Established Receptor?	Source	Reference
Aji_GE_EIP16 (Aji_GE)	Demerecviridae	No	Intesti Bacteriophage formulation M2-601	This study.
Br60	Autographiviridae	“Rough LPS <i>Salmonella</i> ”	<i>Salmonella</i> Genetic Stock Center (SGSC)	(Wilkinson et al., 1972)
Chi	Siphoviridae	Flagella	Gift from Jason Gill	(Samuel et al., 1999; Schade et al., 1967)
FelixO1	Myoviridae	Outer core LPS	Félix d'Hérelle Reference Center for Bacterial Viruses	(Gebhart et al., 2017; Lindberg and Hellerqvist, 1971; Tu et al., 2017)
Ffm	Autographiviridae	“Rough-LPS <i>Salmonella</i> ”	<i>Salmonella</i> Genetic Stock Center (SGSC)	(Graña et al., 1985; Lee et al., 2013; Lindberg and Hellerqvist, 1971; MacPhee et al., 1975; Marti et al., 2013; Schwartz, 1980; Wilkinson et al., 1972; Wright et al., 1980)
P22	Podoviridae	O-Antigen LPS	Gift from Richard Calendar	(Bohm et al., 2018; Steinbacher et al., 1997; Wright et al., 1980)
Reaper_GE_8C2 (Reaper_GE)	Siphoviridae	No	Intesti Bacteriophage formulation M2-601	This study
S16	Myoviridae	OmpC	Félix d'Hérelle Reference Center for Bacterial Viruses	(Marti et al., 2013)
Savina_GE_6H2 (Savina_GE)	Myoviridae	No	Intesti Bacteriophage formulation M2-601	This study
Shishito_GE_6F2 (Shishito_GE)	Autographiviridae	No	Intesti Bacteriophage formulation M2-601	This study
SP6	Autographiviridae	O-Antigen LPS	Gift from Ian J Molineaux	(Tu et al., 2017; Wright et al., 1980)

1050 **References:**

- 1051 • Abedon, S.T. (2009). Chapter 1 Phage Evolution and Ecology. In *Advances in Applied*
1052 *Microbiology*, (Academic Press), pp. 1–45.
- 1053 • Arkin, A.P., Cottingham, R.W., Henry, C.S., Harris, N.L., Stevens, R.L., Maslov, S., Dehal, P.,
1054 Ware, D., Perez, F., Canon, S., et al. (2018). KBase: The United States Department of
1055 Energy Systems Biology Knowledgebase. *Nat. Biotechnol.* *36*, 566–569.
- 1056 • Arndt, D., Grant, J.R., Marcu, A., Sajed, T., Pon, A., Liang, Y., and Wishart, D.S. (2016).
1057 PHASTER: a better, faster version of the PHAST phage search tool. *Nucleic Acids Res.* *44*,
1058 W16–W21.
- 1059 • Aurass, P., Düvel, J., Karste, S., Nübel, U., Rabsch, W., and Flieger, A. (2018). glnA
1060 Truncation in *Salmonella enterica* Results in a Small Colony Variant Phenotype, Attenuated
1061 Host Cell Entry, and Reduced Expression of Flagellin and SPI-1-Associated Effector Genes.
1062 *Appl. Environ. Microbiol.* *84*, 3687.
- 1063 • Bai, J., Jeon, B., and Ryu, S. (2019). Effective inhibition of *Salmonella* Typhimurium in fresh
1064 produce by a phage cocktail targeting multiple host receptors. *Food Microbiol.* *77*, 52–60.
- 1065 • Barrangou, R., and Oost, J. (2014). Bacteriophage exclusion, a new defense system. *EMBO*
1066 *J.* *34*, 134–135.
- 1067 • Battesti, A., Majdalani, N., and Gottesman, S. (2011). The RpoS-mediated general stress
1068 response in *Escherichia coli*. *Annu. Rev. Microbiol.* *65*, 189–213.
- 1069 • Battesti, A., Majdalani, N., and Gottesman, S. (2015). Stress sigma factor RpoS degradation
1070 and translation are sensitive to the state of central metabolism. *Proc. Natl. Acad. Sci. U. S. A.*
1071 *112*, 5159–5164.
- 1072 • Beltran, P., Plock, S.A., Smith, N.H., Whittam, T.S., Old, D.C., and Selander, R.K. (1991).
1073 Reference collection of strains of the *Salmonella typhimurium* complex from natural
1074 populations. *J. Gen. Microbiol.* *137*, 601–606.
- 1075 • Bernheim, A., and Sorek, R. (2020). The pan-immune system of bacteria: antiviral defence as
1076 a community resource. *Nat. Rev. Microbiol.* *18*, 113–119.
- 1077 • Betts, A., Gifford, D.R., MacLean, R.C., and King, K.C. (2016). Parasite diversity drives rapid
1078 host dynamics and evolution of resistance in a bacteria-phage system. *Evolution* *70*, 969–
1079 978.
- 1080 • Bohm, K., Porwollik, S., Chu, W., Dover, J.A., Gilcrease, E.B., Casjens, S.R., McClelland, M.,
1081 and Parent, K.N. (2018). Genes affecting progression of bacteriophage P22 infection in
1082 *Salmonella* identified by transposon and single gene deletion screens. *Mol. Microbiol.* *108*,
1083 288–305.
- 1084 • Bolger, A.M., Lohse, M., and Usadel, B. (2014). Trimmomatic: a flexible trimmer for Illumina
1085 sequence data. *Bioinformatics* *30*, 2114–2120.
- 1086 • Bondy-Denomy, J., Qian, J., Westra, E.R., Buckling, A., Guttman, D.S., Davidson, A.R., and
1087 Maxwell, K.L. (2016). Prophages mediate defense against phage infection through diverse
1088 mechanisms. *ISME J.* *10*, 2854–2866.
- 1089 • Brandão, A., Pires, D.P., Coppens, L., Voet, M., Lavigne, R., and Azeredo, J. (2021).
1090 Differential transcription profiling of the phage LUZ19 infection process in different growth
1091 media. *RNA Biol.* 1–13.
- 1092 • Breitbart, M., and Rohwer, F. (2005). Here a virus, there a virus, everywhere the same virus?
1093 *Trends Microbiol.* *13*, 278–284.
- 1094 • Broadbent, S.E., Davies, M.R., and van der Woude, M.W. (2010). Phase variation controls
1095 expression of *Salmonella* lipopolysaccharide modification genes by a DNA methylation-
1096 dependent mechanism. *Mol. Microbiol.* *77*, 337–353.
- 1097 • Brüssow, H. (2013). Bacteriophage-host interaction: from splendid isolation into a messy

- 1098 reality. *Curr. Opin. Microbiol.* *16*, 500–506.
- 1099 • Buchfink, B., Xie, C., and Huson, D.H. (2015). Fast and sensitive protein alignment using
1100 DIAMOND. *Nat. Methods* *12*, 59–60.
- 1101 • Burgin, A.B., Parodos, K., Lane, D.J., and Pace, N.R. (1990). The excision of intervening
1102 sequences from *Salmonella* 23S ribosomal RNA. *Cell* *60*, 405–414.
- 1103 • Calendar, R. (2012). *The Bacteriophages: Volume 1* (Springer Science & Business Media).
- 1104 • Camacho, C., Coulouris, G., Avagyan, V., Ma, N., Papadopoulos, J., Bealer, K., and Madden,
1105 T.L. (2009). BLAST+: architecture and applications. *BMC Bioinformatics* *10*, 421.
- 1106 • Campbell, A. (2003). The future of bacteriophage biology. *Nat. Rev. Genet.* *4*, 471–477.
- 1107 • Canals, R., Hammarlöf, D.L., Kröger, C., Owen, S.V., Fong, W.Y., Lacharme-Lora, L., Zhu,
1108 X., Wenner, N., Carden, S.E., Honeycutt, J., et al. (2019). Adding function to the genome of
1109 African *Salmonella* Typhimurium ST313 strain D23580. *PLoS Biol.* *17*, e3000059.
- 1110 • Carim, S., Azadeh, A.L., Kazakov, A.E., Price, M.N., Walian, P.J., Chakraborty, R.,
1111 Deutschbauer, A.M., Mutalik, V.K., and Arkin, A.P. (2020). Systematic Discovery of
1112 *Pseudomonas* Genetic Factors Involved in Sensitivity to Tailocins.
- 1113 • Casjens, S.R., and Hendrix, R.W. (2015). Bacteriophage lambda: Early pioneer and still
1114 relevant. *Virology* *479-480*, 310–330.
- 1115 • Chan, B.K., and Turner, P.E. (2020). High-throughput discovery of phage receptors using
1116 transposon insertion sequencing of bacteria. *Proceedings of the*
- 1117 • Chan, B.K., Abedon, S.T., and Loc-Carrillo, C. (2013). Phage cocktails and the future of
1118 phage therapy. *Future Microbiol.* *8*, 769–783.
- 1119 • Chan, B.K., Siström, M., Wertz, J.E., Kortright, K.E., Narayan, D., and Turner, P.E. (2016).
1120 Phage selection restores antibiotic sensitivity in MDR *Pseudomonas aeruginosa*. *Sci. Rep.* *6*,
1121 26717.
- 1122 • Chan, B.K., Turner, P.E., Kim, S., Mojibian, H.R., Eleftheriades, J.A., and Narayan, D. (2018).
1123 Phage treatment of an aortic graft infected with *Pseudomonas aeruginosa*. *Evolution,*
1124 *Medicine, and Public Health* *2018*, 60–66.
- 1125 • Chaumeil, P.-A., Mussig, A.J., Hugenholtz, P., and Parks, D.H. (2019). GTDB-Tk: a toolkit to
1126 classify genomes with the Genome Taxonomy Database. *Bioinformatics*.
- 1127 • Chen, C.Y., Buchmeier, N.A., Libby, S., Fang, F.C., Krause, M., and Guiney, D.G. (1995).
1128 Central regulatory role for the RpoS sigma factor in expression of *Salmonella* dublin plasmid
1129 virulence genes. *J. Bacteriol.* *177*, 5303–5309.
- 1130 • Chirakadze, I., Perets, A., and Ahmed, R. (2009). Phage Typing. *Methods in Molecular*
1131 *Biology* 293–305.
- 1132 • Cho, S.-H., Szewczyk, J., Pesavento, C., Zietek, M., Banzhaf, M., Roszczenko, P., Asmar,
1133 A., Laloux, G., Hov, A.-K., Leverrier, P., et al. (2014). Detecting envelope stress by
1134 monitoring β -barrel assembly. *Cell* *159*, 1652–1664.
- 1135 • Christen, M., Beusch, C., Bösch, Y., Cerletti, D., Flores-Tinoco, C.E., Del Medico, L., Tschan,
1136 F., and Christen, B. (2016). Quantitative Selection Analysis of Bacteriophage ϕ CbK
1137 Susceptibility in *Caulobacter crescentus*. *J. Mol. Biol.* *428*, 419–430.
- 1138 • Cota, I., Sánchez-Romero, M.A., Hernández, S.B., Graciela Pucciarelli, M., Portillo, F.G., and
1139 Casadesús, J. (2015). Epigenetic Control of *Salmonella enterica* O-Antigen Chain Length: A
1140 Tradeoff between Virulence and Bacteriophage Resistance. *PLOS Genetics* *11*, e1005667.
- 1141 • Cowley, L.A., Low, A.S., Pickard, D., Boinett, C.J., Dallman, T.J., Day, M., Perry, N., Gally,
1142 D.L., Parkhill, J., Jenkins, C., et al. (2018). Transposon Insertion Sequencing Elucidates
1143 Novel Gene Involvement in Susceptibility and Resistance to Phages T4 and T7 in
1144 *Escherichia coli* O157. *MBio* *9*.
- 1145 • Crawford, R.W., Keestra, A.M., Winter, S.E., Xavier, M.N., Tsolis, R.M., Tolstikov, V., and

- 1146 Bäumler, A.J. (2012). Very long O-antigen chains enhance fitness during Salmonella-induced
1147 colitis by increasing bile resistance. *PLoS Pathog.* 8, e1002918.
- 1148 • Davies, M.R., Broadbent, S.E., Harris, S.R., Thomson, N.R., and van der Woude, M.W.
1149 (2013). Horizontally acquired glycosyltransferase operons drive salmonellae
1150 lipopolysaccharide diversity. *PLoS Genet.* 9, e1003568.
- 1151 • Dedrick, R.M., Jacobs-Sera, D., Bustamante, C.A.G., Garlena, R.A., Mavrich, T.N., Pope,
1152 W.H., Reyes, J.C.C., Russell, D.A., Adair, T., Alvey, R., et al. (2017). Prophage-mediated
1153 defence against viral attack and viral counter-defence. *Nat Microbiol* 2, 16251.
- 1154 • De Smet, J., Hendrix, H., Blasdel, B.G., Danis-Wlodarczyk, K., and Lavigne, R. (2017).
1155 *Pseudomonas* predators: understanding and exploiting phage-host interactions. *Nat. Rev.*
1156 *Microbiol.* 15, 517–530.
- 1157 • Díaz-Muñoz, S.L., and Koskella, B. (2014). Bacteria-phage interactions in natural
1158 environments. *Adv. Appl. Microbiol.* 89, 135–183.
- 1159 • Domínguez-Medina, C.C., Pérez-Toledo, M., Schager, A.E., Marshall, J.L., Cook, C.N.,
1160 Bobat, S., Hwang, H., Chun, B.J., Logan, E., Bryant, J.A., et al. (2020). Outer membrane
1161 protein size and LPS O-antigen define protective antibody targeting to the Salmonella
1162 surface. *Nat. Commun.* 11, 851.
- 1163 • Dong, T., and Schellhorn, H.E. (2010). Role of RpoS in virulence of pathogens. *Infect.*
1164 *Immun.* 78, 887–897.
- 1165 • Dy, R.L., Richter, C., Salmond, G.P.C., and Fineran, P.C. (2014). Remarkable Mechanisms
1166 in Microbes to Resist Phage Infections. *Annu Rev Virol* 1, 307–331.
- 1167 • Fang, F.C., Libby, S.J., Buchmeier, N.A., Loewen, P.C., Switala, J., Harwood, J., and Guiney,
1168 D.G. (1992). The alternative sigma factor katF (rpoS) regulates Salmonella virulence. *Proc.*
1169 *Natl. Acad. Sci. U. S. A.* 89, 11978–11982.
- 1170 • Fu, S., Octavia, S., Tanaka, M.M., Sintchenko, V., and Lan, R. (2015). Defining the Core
1171 Genome of Salmonella enterica Serovar Typhimurium for Genomic Surveillance and
1172 Epidemiological Typing. *J. Clin. Microbiol.* 53, 2530–2538.
- 1173 • Fu, S., Hiley, L., Octavia, S., Tanaka, M.M., Sintchenko, V., and Lan, R. (2017). Comparative
1174 genomics of Australian and international isolates of Salmonella Typhimurium: correlation of
1175 core genome evolution with CRISPR and prophage profiles. *Sci. Rep.* 7, 9733.
- 1176 • Gao, R., Naushad, S., Moineau, S., Levesque, R., Goodridge, L., and Ogunremi, D. (2020).
1177 Comparative genomic analysis of 142 bacteriophages infecting Salmonella enterica subsp.
1178 enterica. *BMC Genomics* 21, 374.
- 1179 • Garneau, J.R., Depardieu, F., Fortier, L.-C., Bikard, D., and Monot, M. (2017). PhageTerm: a
1180 tool for fast and accurate determination of phage termini and packaging mechanism using
1181 next-generation sequencing data. *Sci. Rep.* 7, 8292.
- 1182 • Gautreau, G., Bazin, A., Gachet, M., Planel, R., Burlot, L., Dubois, M., Perrin, A., Médigue,
1183 C., Calteau, A., Cruveiller, S., et al. (2020). PPanGGOLiN: Depicting microbial diversity via a
1184 partitioned pangenome graph. *PLoS Comput. Biol.* 16, e1007732.
- 1185 • Gebhart, D., Williams, S.R., and Scholl, D. (2017). Bacteriophage SP6 encodes a second
1186 tailspike protein that recognizes Salmonella enterica serogroups C2 and C3. *Virology* 507,
1187 263–266.
- 1188 • Goosen, N., and Putte, P. (1995). The regulation of transcription initiation by integration host
1189 factor. *Mol. Microbiol.* 16, 1–7.
- 1190 • Gordillo Altamirano, F.L., and Barr, J.J. (2019). Phage Therapy in the Postantibiotic Era. *Clin.*
1191 *Microbiol. Rev.* 32.
- 1192 • Gordillo Altamirano, F., Forsyth, J.H., Patwa, R., Kostoulas, X., Trim, M., Subedi, D., Archer,
1193 S.K., Morris, F.C., Oliveira, C., Kielty, L., et al. (2021). Bacteriophage-resistant Acinetobacter

- 1194 baumannii are resensitized to antimicrobials. *Nat Microbiol* 6, 157–161.
- 1195 • Graña, D., Youderian, P., and Susskind, M.M. (1985). Mutations that improve the ant
1196 promoter of Salmonella phage P22. *Genetics* 110, 1–16.
- 1197 • Heinrichs, D.E., Yethon, J.A., and Whitfield, C. (1998). Molecular basis for structural diversity
1198 in the core regions of the lipopolysaccharides of Escherichia coli and Salmonella enterica.
1199 *Mol. Microbiol.* 30, 221–232.
- 1200 • Heller, K., and Braun, V. (1982). Polymannose O-antigens of Escherichia coli. *J. Virol.* 41,
1201 222–227.
- 1202 • Hengge-Aronis, R. (2002). Signal Transduction and Regulatory Mechanisms Involved in
1203 Control of the σ S (RpoS) Subunit of RNA Polymerase. *Microbiol. Mol. Biol. Rev.* 66, 373–
1204 395.
- 1205 • Hesse, S., Rajaure, M., Wall, E., Johnson, J., Bliskovsky, V., Gottesman, S., and Adhya, S.
1206 (2020). Phage Resistance in Multidrug-Resistant Klebsiella pneumoniae ST258 Evolves via
1207 Diverse Mutations That Culminate in Impaired Adsorption. *MBio* 11.
- 1208 • Hoare, A., Bittner, M., Carter, J., Alvarez, S., Zaldívar, M., Bravo, D., Valvano, M.A., and
1209 Contreras, I. (2006). The outer core lipopolysaccharide of Salmonella enterica serovar Typhi
1210 is required for bacterial entry into epithelial cells. *Infect. Immun.* 74, 1555–1564.
- 1211 • Holmfeldt, K., Middelboe, M., Nybroe, O., and Riemann, L. (2007). Large variabilities in host
1212 strain susceptibility and phage host range govern interactions between lytic marine phages
1213 and their Flavobacterium hosts. *Appl. Environ. Microbiol.* 73, 6730–6739.
- 1214 • van Houte, S., Buckling, A., and Westra, E.R. (2016). Evolutionary Ecology of Prokaryotic
1215 Immune Mechanisms. *Microbiol. Mol. Biol. Rev.* 80, 745–763.
- 1216 • Howard-Varona, C., Hargreaves, K.R., Solonenko, N.E., Markillie, L.M., White, R.A., 3rd,
1217 Brewer, H.M., Ansong, C., Orr, G., Adkins, J.N., and Sullivan, M.B. (2018). Multiple
1218 mechanisms drive phage infection efficiency in nearly identical hosts. *ISME J.* 12, 1605–
1219 1618.
- 1220 • Hudson, H.P., Microbiology, A.A.L., and 1978 (1978). Lipopolysaccharide core defects in
1221 Salmonella typhimurium mutants which are resistant to Felix O phage but retain smooth
1222 character. *Mic.microbiologyresearch.org* 109, 97–112.
- 1223 • Hyman, P., and Abedon, S.T. (2010). Chapter 7 - Bacteriophage Host Range and Bacterial
1224 Resistance. In *Advances in Applied Microbiology*, (Academic Press), pp. 217–248.
- 1225 • Ibanez-Ruiz, M., Robbe-Saule, V., Hermant, D., Labrude, S., and Norel, F. (2000).
1226 Identification of RpoS (σ (S))-regulated genes in Salmonella enterica serovar
1227 typhimurium. *J. Bacteriol.* 182, 5749–5756.
- 1228 • Islam, M.S., Zhou, Y., Liang, L., Nime, I., Liu, K., Yan, T., Wang, X., and Li, J. (2019).
1229 Application of a Phage Cocktail for Control of Salmonella in Foods and Reducing Biofilms.
1230 *Viruses* 11.
- 1231 • de Jonge, P.A., Nobrega, F.L., Brouns, S.J.J., and Dutilh, B.E. (2019). Molecular and
1232 Evolutionary Determinants of Bacteriophage Host Range. *Trends Microbiol.* 27, 51–63.
- 1233 • Karam, J.D., and Drake, J.W. (1994). *Molecular biology of bacteriophage* (American Society
1234 for Microbiology).
- 1235 • Katoh, K., and Standley, D.M. (2014). MAFFT: iterative refinement and additional methods.
1236 *Methods Mol. Biol.* 1079, 131–146.
- 1237 • Keen, E.C., and Adhya, S.L. (2015). Phage Therapy: Current Research and Applications.
1238 *Clin. Infect. Dis.* 61, 141–142.
- 1239 • Kim, M., and Ryu, S. (2012). Spontaneous and transient defence against bacteriophage by
1240 phase-variable glucosylation of O-antigen in Salmonella enterica serovar Typhimurium. *Mol.*
1241 *Microbiol.* 86, 411–425.

- 1242 • Kim, D., Paggi, J.M., Park, C., Bennett, C., and Salzberg, S.L. (2019). Graph-based genome
1243 alignment and genotyping with HISAT2 and HISAT-genotype. *Nat. Biotechnol.* **37**, 907–915.
- 1244 • Klose, K.E., and Mekalanos, J.J. (1997). Simultaneous prevention of glutamine synthesis and
1245 high-affinity transport attenuates *Salmonella typhimurium* virulence. *Infect. Immun.* **65**, 587–
1246 596.
- 1247 • Kong, Q., Yang, J., Liu, Q., Alamuri, P., Roland, K.L., and Curtiss, R., 3rd (2011). Effect of
1248 deletion of genes involved in lipopolysaccharide core and O-antigen synthesis on virulence
1249 and immunogenicity of *Salmonella enterica* serovar typhimurium. *Infect. Immun.* **79**, 4227–
1250 4239.
- 1251 • Kortright, K.E., Chan, B.K., Koff, J.L., and Turner, P.E. (2019). Phage Therapy: A Renewed
1252 Approach to Combat Antibiotic-Resistant Bacteria. *Cell Host Microbe* **25**, 219–232.
- 1253 • Kortright, K.E., Chan, B.K., and Turner, P.E. (2020). High-throughput discovery of phage
1254 receptors using transposon insertion sequencing of bacteria. *Proc. Natl. Acad. Sci. U. S. A.*
1255 **117**, 18670–18679.
- 1256 • Koskella, B., and Taylor, T.B. (2018). Multifaceted Impacts of Bacteriophages in the Plant
1257 Microbiome. *Annu. Rev. Phytopathol.* **56**, 361–380.
- 1258 • Kutter, E., and Sulakvelidze, A. (2004). *Bacteriophages: Biology and Applications* (CRC
1259 Press).
- 1260 • Lago, M., Monteil, V., Douche, T., Guglielmini, J., Criscuolo, A., Maufrais, C., Matondo, M.,
1261 and Norel, F. (2017). Proteome remodelling by the stress sigma factor RpoS/ σ S in
1262 *Salmonella*: identification of small proteins and evidence for post-transcriptional regulation.
1263 *Sci. Rep.* **7**, 2127.
- 1264 • Lee, J.-H., Shin, H., Choi, Y., and Ryu, S. (2013). Complete genome sequence analysis of
1265 bacterial-flagellum-targeting bacteriophage chi. *Arch. Virol.* **158**, 2179–2183.
- 1266 • Lenski, R.E. (1988). Dynamics of Interactions between Bacteria and Virulent Bacteriophage.
1267 In *Advances in Microbial Ecology*, K.C. Marshall, ed. (Boston, MA: Springer US), pp. 1–44.
- 1268 • Letunic, I., and Bork, P. (2019). Interactive Tree Of Life (iTOL) v4: recent updates and new
1269 developments. *Nucleic Acids Res.* **47**, W256–W259.
- 1270 • Lévi-Meyrueis, C., Monteil, V., Sismeiro, O., Dillies, M.-A., Monot, M., Jagla, B., Coppée, J.-
1271 Y., Dupuy, B., and Norel, F. (2014). Expanding the RpoS/ σ S-Network by RNA Sequencing
1272 and Identification of σ S-Controlled Small RNAs in *Salmonella*. *PLoS One* **9**, e96918–12.
- 1273 • Lindberg, A.A., and Hellerqvist, C.G. (1971). Bacteriophage attachment sites, serological
1274 specificity, and chemical composition of the lipopolysaccharides of semirough and rough
1275 mutants of *Salmonella typhimurium*. *J. Bacteriol.* **105**, 57–64.
- 1276 • Liu, H., Price, M.N., Waters, R.J., Ray, J., Carlson, H.K., Lamson, J.S., Chakraborty, R.,
1277 Arkin, A.P., and Deutschbauer, A.M. (2018). Magic Pools: Parallel Assessment of
1278 Transposon Delivery Vectors in Bacteria. *mSystems* **3**.
- 1279 • Love, M.I., Huber, W., and Anders, S. (2014). Moderated estimation of fold change and
1280 dispersion for RNA-seq data with DESeq2. *Genome Biol.* **15**, 550.
- 1281 • Lucchini, S., McDermott, P., Thompson, A., and Hinton, J.C.D. (2009). The H-NS-like protein
1282 StpA represses the RpoS (σ 38) regulon during exponential growth of *Salmonella*
1283 *Typhimurium*. *Mol. Microbiol.* **74**, 1169–1186.
- 1284 • MacPhee, D.G., Krishnapillai, V., Roantree, R.J., and Stocker, B.A. (1975). Mutations in
1285 *Salmonella typhimurium* conferring resistance to Felix O phage without loss of smooth
1286 character. *J. Gen. Microbiol.* **87**, 1–10.
- 1287 • Macculloch, B., Hoffmann, S., and Batz, M. (2015). *Economic Burden of Major Foodborne*
1288 *Illnesses Acquired in the United States* (CreateSpace Independent Publishing Platform).
- 1289 • Mangalea, M.R., and Duerkop, B.A. (2020). Fitness Trade-Offs Resulting from Bacteriophage

- 1290 Resistance Potentiate Synergistic Antibacterial Strategies. *Infect. Immun.* **88**.
- 1291 • Marçais, G., Delcher, A.L., Phillippy, A.M., Coston, R., Salzberg, S.L., and Zimin, A. (2018).
- 1292 MUMmer4: A fast and versatile genome alignment system. *PLoS Comput. Biol.* **14**,
- 1293 e1005944.
- 1294 • Mariscotti, J.F., and García-del Portillo, F. (2009). Genome expression analyses revealing
- 1295 the modulation of the Salmonella Rcs regulon by the attenuator IgaA. *J. Bacteriol.* **191**,
- 1296 1855–1867.
- 1297 • Marti, R., Zurfluh, K., Hagens, S., Pianezzi, J., Klumpp, J., and Loessner, M.J. (2013). Long
- 1298 tail fibres of the novel broad-host-range T-even bacteriophage S16 specifically
- 1299 recognize Salmonella OmpC. *Molecular Microbiology* **87**, 818–834.
- 1300 • McCallin, S., Sarker, S.A., Sultana, S., Oechslin, F., and Brüssow, H. (2018). Metagenome
- 1301 analysis of Russian and Georgian Pyophage cocktails and a placebo-controlled safety trial of
- 1302 single phage versus phage cocktail in healthy Staphylococcus aureus carriers. *Environ.*
- 1303 *Microbiol.* **20**, 3278–3293.
- 1304 • Medalla, F., Gu, W., Mahon, B.E., Judd, M., Folster, J., Griffin, P.M., and Hoekstra, R.M.
- 1305 (2016). Estimated Incidence of Antimicrobial Drug-Resistant Nontyphoidal Salmonella
- 1306 Infections, United States, 2004-2012. *Emerg. Infect. Dis.* **23**, 29–37.
- 1307 • Mirzaei, M.K., and Maurice, C.F. (2017). Ménage à trois in the human gut: interactions
- 1308 between host, bacteria and phages. *Nat. Rev. Microbiol.* **15**, 397–408.
- 1309 • Molineux, I. (2002). T7 Bacteriophages. *Encyclopedia of Molecular Biology*.
- 1310 • Moller, A.G., Lindsay, J.A., and Read, T.D. (2019). Determinants of Phage Host Range in
- 1311 Staphylococcus Species. *Appl. Environ. Microbiol.* **85**.
- 1312 • Mutalik, V.K., Novichkov, P.S., Price, M.N., Owens, T.K., Callaghan, M., Carim, S.,
- 1313 Deutschbauer, A.M., and Arkin, A.P. (2019). Dual-barcoded shotgun expression library
- 1314 sequencing for high-throughput characterization of functional traits in bacteria. *Nat. Commun.*
- 1315 **10**, 308.
- 1316 • Mutalik, V.K., Adler, B.A., Rishi, H.S., Piya, D., Zhong, C., Koskella, B., Calendar, R.,
- 1317 Novichkov, P., Price, M.N., Deutschbauer, A.M., et al. (2020). High-throughput mapping of
- 1318 the phage resistance landscape in *E. coli*.
- 1319 • Nagy, G., Danino, V., Dobrindt, U., Pallen, M., Chaudhuri, R., Emödy, L., Hinton, J.C., and
- 1320 Hacker, J. (2006). Down-regulation of key virulence factors makes the Salmonella enterica
- 1321 serovar Typhimurium rfaH mutant a promising live-attenuated vaccine candidate. *Infect.*
- 1322 *Immun.* **74**, 5914–5925.
- 1323 • Nickerson, C.A., and Curtiss, R., 3rd (1997). Role of sigma factor RpoS in initial stages of
- 1324 Salmonella typhimurium infection. *Infect. Immun.* **65**, 1814–1823.
- 1325 • Nobrega, F.L., Vlot, M., de Jonge, P.A., Dreesens, L.L., Beaumont, H.J.E., Lavigne, R.,
- 1326 Dutilh, B.E., and Brouns, S.J.J. (2018). Targeting mechanisms of tailed bacteriophages. *Nat.*
- 1327 *Rev. Microbiol.* **16**, 760–773.
- 1328 • Nurk, S., Bankevich, A., Antipov, D., Gurevich, A., Korobeynikov, A., Lapidus, A., Prjibelsky,
- 1329 A., Pyshkin, A., Sirotkin, A., Sirotkin, Y., et al. (2013). Assembling Genomes and Mini-
- 1330 metagenomes from Highly Chimeric Reads. In *Research in Computational Molecular Biology*,
- 1331 (Springer Berlin Heidelberg), pp. 158–170.
- 1332 • Owen, S.V., Wenner, N., Dulberger, C.L., and Rodwell, E.V. (2020). Prophage-encoded
- 1333 phage defence proteins with cognate self-immunity. *bioRxiv*.
- 1334 • Perteza, M., Perteza, G.M., Antonescu, C.M., Chang, T.-C., Mendell, J.T., and Salzberg, S.L.
- 1335 (2015). StringTie enables improved reconstruction of a transcriptome from RNA-seq reads.
- 1336 *Nat. Biotechnol.* **33**, 290–295.
- 1337 • Petsong, K., Benjakul, S., Chaturongakul, S., Switt, A.I.M., and Vongkamjan, K. (2019). Lysis

- 1338 Profiles of Salmonella Phages on Salmonella Isolates from Various Sources and Efficiency of
1339 a Phage Cocktail against *S. Enteritidis* and *S. Typhimurium*. *Microorganisms* 7.
- 1340 • Pickard, D., Kingsley, R.A., Hale, C., Turner, K., Sivaraman, K., Wetter, M., Langridge, G.,
1341 and Dougan, G. (2013). A genomewide mutagenesis screen identifies multiple genes
1342 contributing to Vi capsular expression in *Salmonella enterica* serovar Typhi. *J. Bacteriol.* 195,
1343 1320–1326.
- 1344 • Pirnay, J.-P., and Kutter, E. (2020). Bacteriophages: it's a medicine, Jim, but not as we know
1345 it. *Lancet Infect. Dis.*
- 1346 • Porwollik, S., Santiviago, C.A., Cheng, P., Long, F., Desai, P., Fredlund, J., Srikumar, S.,
1347 Silva, C.A., Chu, W., Chen, X., et al. (2014). Defined single-gene and multi-gene deletion
1348 mutant collections in *Salmonella enterica* sv Typhimurium. *PLoS One* 9, e99820.
- 1349 • Price, M.N., Dehal, P.S., and Arkin, A.P. (2010). FastTree 2--approximately maximum-
1350 likelihood trees for large alignments. *PLoS One* 5, e9490.
- 1351 • Price, M.N., Wetmore, K.M., Waters, R.J., Callaghan, M., Ray, J., Liu, H., Kuehl, J.V.,
1352 Melnyk, R.A., Lamson, J.S., Suh, Y., et al. (2018). Mutant phenotypes for thousands of
1353 bacterial genes of unknown function. *Nature* 557, 503–509.
- 1354 • Rabsch, W. (2007). *Salmonella typhimurium* phage typing for pathogens. *Methods Mol. Biol.*
1355 394, 177–211.
- 1356 • Richardson, E.J., Limaye, B., Inamdar, H., Datta, A., Manjari, K.S., Pullinger, G.D., Thomson,
1357 N.R., Joshi, R.R., Watson, M., and Stevens, M.P. (2011). Genome sequences of *Salmonella*
1358 *enterica* serovar typhimurium, Choleraesuis, Dublin, and Gallinarum strains of well- defined
1359 virulence in food-producing animals. *J. Bacteriol.* 193, 3162–3163.
- 1360 • Rishi, H.S., Toro, E., Liu, H., Wang, X., Qi, L.S., and Arkin, A.P. (2020). Systematic genome-
1361 wide querying of coding and non-coding functional elements in *E. coli* using CRISPRi.
- 1362 • Roantree, R.J., Kuo, T.T., and MacPhee, D.G. (1977). The effect of defined
1363 lipopolysaccharide core defects upon antibiotic resistances of *Salmonella typhimurium*. *J.*
1364 *Gen. Microbiol.* 103, 223–234.
- 1365 • Robbe-Saule, V., Coynault, C., and Norel, F. (1995). The live oral typhoid vaccine Ty21a is a
1366 *rpoS* mutant and is susceptible to various environmental stresses. *FEMS Microbiol. Lett.* 126,
1367 171–176.
- 1368 • Roberts, R.J., Vincze, T., Posfai, J., and Macelis, D. (2015). REBASE--a database for DNA
1369 restriction and modification: enzymes, genes and genomes. *Nucleic Acids Res.* 43, D298–
1370 D299.
- 1371 • Rostøl, J.T., and Marraffini, L. (2019). (Ph)ighting Phages: How Bacteria Resist Their
1372 Parasites. *Cell Host Microbe* 25, 184–194.
- 1373 • Rousset, F., Cui, L., Siouve, E., Becavin, C., Depardieu, F., and Bikard, D. (2018). Genome-
1374 wide CRISPR-dCas9 screens in *E. coli* identify essential genes and phage host factors. *PLoS*
1375 *Genet.* 14, e1007749.
- 1376 • Samson, J.E., Magadán, A.H., Sabri, M., and Moineau, S. (2013). Revenge of the phages:
1377 defeating bacterial defences. *Nat. Rev. Microbiol.* 11, 675–687.
- 1378 • Samuel, A.D., Pitta, T.P., Ryu, W.S., Danese, P.N., Leung, E.C., and Berg, H.C. (1999).
1379 Flagellar determinants of bacterial sensitivity to chi-phage. *Proceedings of the National*
1380 *Academy of Sciences* 96, 9863–9866.
- 1381 • Samuels, D.J., Frye, J.G., Porwollik, S., McClelland, M., Mrázek, J., Hoover, T.R., and Karls,
1382 A.C. (2013). Use of a promiscuous, constitutively-active bacterial enhancer-binding protein to
1383 define the σ^{54} (RpoN) regulon of *Salmonella Typhimurium* LT2. *BMC Genomics* 14, 602.
- 1384 • Sanderson, K.E., MacAlister, T., Costerton, J.W., and Cheng, K.J. (1974). Permeability of
1385 lipopolysaccharide-deficient (rough) mutants of *Salmonella typhimurium* to antibiotics,

- 1386 lysozyme, and other agents. *Can. J. Microbiol.* *20*, 1135–1145.
- 1387 • Sawitzke, J.A., Thomason, L.C., Costantino, N., Bubunenko, M., Datta, S., and Court, D.L.
1388 (2007). Recombineering: In Vivo Genetic Engineering in *E. coli*, *S. enterica*, and Beyond. In
1389 *Methods in Enzymology*, (Academic Press), pp. 171–199.
- 1390 • Schade, S.Z., Adler, J., and Ris, H. (1967). How bacteriophage chi attacks motile bacteria. *J.*
1391 *Virol.* *1*, 599–609.
- 1392 • Schwartz, M. (1980). Interaction of Phages with their Receptor Proteins. In *Virus Receptors:*
1393 *Part 1 Bacterial Viruses*, L.L. Randall, and L. Philipson, eds. (Dordrecht: Springer
1394 Netherlands), pp. 59–94.
- 1395 • Seif, Y., Monk, J.M., Machado, H., Kavvas, E., and Palsson, B.O. (2019). Systems Biology
1396 and Pangenome of *Salmonella* O-Antigens. *MBio* *10*.
- 1397 • Shariat, N., Timme, R.E., Pettengill, J.B., Barrangou, R., and Dudley, E.G. (2015).
1398 Characterization and evolution of *Salmonella* CRISPR-Cas systems. *Microbiology* *161*, 374–
1399 386.
- 1400 • Shin, H., Lee, J.-H., Kim, H., Choi, Y., Heu, S., and Ryu, S. (2012). Receptor diversity and
1401 host interaction of bacteriophages infecting *Salmonella enterica* serovar Typhimurium. *PLoS*
1402 *One* *7*, e43392.
- 1403 • Shkoporov, A.N., and Hill, C. (2019). Bacteriophages of the Human Gut: The “Known
1404 Unknown” of the Microbiome. *Cell Host Microbe* *25*, 195–209.
- 1405 • Slauch, J.M., Lee, A.A., Mahan, M.J., and Mekalanos, J.J. (1996). Molecular characterization
1406 of the *oafA* locus responsible for acetylation of *Salmonella typhimurium* O-antigen: *oafA* is a
1407 member of a family of integral membrane trans-acylases. *J. Bacteriol.* *178*, 5904–5909.
- 1408 • Steinbacher, S., Miller, S., Baxa, U., Budisa, N., Weintraub, A., Seckler, R., and Huber, R.
1409 (1997). Phage P22 tailspike protein: crystal structure of the head-binding domain at 2.3 Å,
1410 fully refined structure of the endorhamnosidase at 1.56 Å resolution, and the molecular basis
1411 of O-antigen recognition and cleavage. *J. Mol. Biol.* *267*, 865–880.
- 1412 • Su, J., Gong, H., Lai, J., Main, A., and Lu, S. (2009). The potassium transporter Trk and
1413 external potassium modulate *Salmonella enterica* protein secretion and virulence. *Infect.*
1414 *Immun.* *77*, 667–675.
- 1415 • Suttle, C.A. (2007). Marine viruses—major players in the global ecosystem. *Nat. Rev.*
1416 *Microbiol.* *5*, 801–812.
- 1417 • Tanji, Y., Shimada, T., Yoichi, M., Miyana, K., Hori, K., and Unno, H. (2004). Toward
1418 rational control of *Escherichia coli* O157:H7 by a phage cocktail. *Applied Microbiology and*
1419 *Biotechnology* *64*, 270–274.
- 1420 • Thibault, D., Jensen, P.A., Wood, S., Qabar, C., Clark, S., Shainheit, M.G., Isberg, R.R., and
1421 van Opijnen, T. (2019). Droplet Tn-Seq combines microfluidics with Tn-Seq for identifying
1422 complex single-cell phenotypes. *Nat. Commun.* *10*, 5729.
- 1423 • Toguchi, A., Siano, M., Burkart, M., and Harshey, R.M. (2000). Genetics of swarming motility
1424 in *Salmonella enterica* serovar typhimurium: critical role for lipopolysaccharide. *J. Bacteriol.*
1425 *182*, 6308–6321.
- 1426 • Trudelle, D.M., Bryan, D.W., Hudson, L.K., and Denes, T.G. (2019). Cross-resistance to
1427 phage infection in *Listeria monocytogenes* serotype 1/2a mutants. *Food Microbiol.* *84*,
1428 103239.
- 1429 • Tu, J., Park, T., Morado, D.R., Hughes, K.T., Molineux, I.J., and Liu, J. (2017). Dual host
1430 specificity of phage SP6 is facilitated by tailspike rotation. *Virology* *507*, 206–215.
- 1431 • (u.s.), C.F.D.C.A.P., and Centers for Disease Control and Prevention (U.S.) (2019). Antibiotic
1432 resistance threats in the United States, 2019.
- 1433 • Vasu, K., and Nagaraja, V. (2013). Diverse functions of restriction-modification systems in

- 1434 addition to cellular defense. *Microbiol. Mol. Biol. Rev.* *77*, 53–72.
- 1435 • Wahl, A., Battesti, A., and Ansaldi, M. (2019). Prophages in *Salmonella enterica*: a driving
1436 force in reshaping the genome and physiology of their bacterial host? *Mol. Microbiol.* *111*,
1437 303–316.
- 1438 • Washizaki, A., Yonesaki, T., and Otsuka, Y. (2016). Characterization of the interactions
1439 between *Escherichia coli* receptors, LPS and OmpC, and bacteriophage T4 long tail fibers.
1440 *Microbiologyopen* *5*, 1003–1015.
- 1441 • Weitz, J.S., Poisot, T., Meyer, J.R., Flores, C.O., Valverde, S., Sullivan, M.B., and Hochberg,
1442 M.E. (2013). Phage-bacteria infection networks. *Trends Microbiol.* *21*, 82–91.
- 1443 • Wetmore, K.M., Price, M.N., Waters, R.J., Lamson, J.S., He, J., Hoover, C.A., Blow, M.J.,
1444 Bristow, J., Butland, G., Arkin, A.P., et al. (2015). Rapid quantification of mutant fitness in
1445 diverse bacteria by sequencing randomly bar-coded transposons. *Am Soc Microbiol* *6*,
1446 e00306–e00315.
- 1447 • Wick, R.R., Judd, L.M., Gorrie, C.L., and Holt, K.E. (2017). Unicycler: Resolving bacterial
1448 genome assemblies from short and long sequencing reads. *PLoS Comput. Biol.* *13*,
1449 e1005595.
- 1450 • Wilkinson, R.G., Gemski, P., Jr, and Stocker, B.A. (1972). Non-smooth mutants of
1451 *Salmonella typhimurium*: differentiation by phage sensitivity and genetic mapping. *J. Gen.*
1452 *Microbiol.* *70*, 527–554.
- 1453 • Wilmes-Riesenberg, M.R., Foster, J.W., and Curtiss, R., 3rd (1997). An altered *rpoS* allele
1454 contributes to the avirulence of *Salmonella typhimurium* LT2. *Infect. Immun.* *65*, 203–210.
- 1455 • Wright, A., McConnell, M., and Kanegasaki, S. (1980). Lipopolysaccharide as a
1456 Bacteriophage Receptor. In *Virus Receptors: Part 1 Bacterial Viruses*, L.L. Randall, and L.
1457 Philipson, eds. (Dordrecht: Springer Netherlands), pp. 27–57.
- 1458 • Wright, R.C.T., Friman, V.-P., Smith, M.C.M., and Brockhurst, M.A. (2018). Cross-resistance
1459 is modular in bacteria–phage interactions. *PLoS Biol.* *16*, e2006057–22.
- 1460 • Wright, R.C.T., Friman, V.-P., Smith, M.C.M., and Brockhurst, M.A. (2019). Resistance
1461 Evolution against Phage Combinations Depends on the Timing and Order of Exposure. *mBio*
1462 *10*.
- 1463 • Yen, M., Cairns, L.S., and Camilli, A. (2017). A cocktail of three virulent bacteriophages
1464 prevents *Vibrio cholerae* infection in animal models. *Nat. Commun.* *8*, 14187.
- 1465 • Young, R., and Gill, J.J. (2015). Phage therapy redux—What is to be done? *Science* *350*,
1466 1163–1164.
- 1467 • Zerbino, D.R., and Birney, E. (2008). Velvet: algorithms for de novo short read assembly
1468 using de Bruijn graphs. *Genome Res.* *18*, 821–829.
- 1469 • Zschach, H., Joensen, K.G., Lindhard, B., Lund, O., Goderdzishvili, M., Chkonia, I., Jgenti,
1470 G., Kvatadze, N., Alavidze, Z., Kutter, E.M., et al. (2015). What Can We Learn from a
1471 Metagenomic Analysis of a Georgian Bacteriophage Cocktail? *Viruses* *7*, 6570–6589.
- 1472
- 1473